

RE-ALIGNING LANGUAGE TO VISUAL OBJECTS WITH AN AGENTIC WORKFLOW

Anonymous authors

Paper under double-blind review

ABSTRACT

Language-based object detection (LOD) aims to align visual objects with language expressions. A large amount of paired data is utilized to improve LOD model generalizations. During the training process, recent studies leverage vision-language models (VLMs) to automatically generate human-like expressions for visual objects, facilitating training data scaling up. In this process, we observe that VLM hallucinations bring inaccurate object descriptions (*e.g.*, object name, color, and shape) to deteriorate VL alignment quality. To reduce VLM hallucinations, we propose an agentic workflow controlled by an LLM to re-align language to visual objects via adaptively adjusting image and text prompts. We name this workflow Real-LOD, which includes planning, tool use, and reflection steps. Given an image with detected objects and VLM raw language expressions, Real-LOD reasons its state automatically and arranges action based on our neural symbolic designs (*i.e.*, planning). The action will adaptively adjust the image and text prompts, and send them to VLMs for object re-description (*i.e.*, tool use). Then, we use another LLM to analyze these refined expressions for feedback. These steps are conducted in a cyclic form to gradually improve language descriptions for re-aligning to visual objects. We construct a dataset that contains a tiny amount of 0.18M images with re-aligned language expression and train a prevalent LOD model to surpass existing LOD methods by around 50% on the standard benchmarks. Our Real-LOD workflow, with automatic VL refinement, reveals a potential to preserve data quality along with scaling up data quantity, which further improves LOD performance from a data-alignment perspective.

1 INTRODUCTION

Aligning language expressions to visual objects has been continuously evolving. Initially, a single noun word is used as a category label (Redmon et al., 2016; Ren et al., 2016; Carion et al., 2020) to connect a visual object. Then, phrases are introduced (Akbari et al., 2019; Li et al., 2022; Gao et al., 2023) to describe objects. Further, referring expressions (Su et al., 2020; Zhang et al., 2022) and complete descriptions (Schulter et al., 2023; Yao et al., 2024) are developed for object detection. Although language evolves from coarse labels to fine-grained expressions, the essence of object detection is to align the language data to visual objects. This alignment is challenging as language expressions become diverse to represent various human intentions. As for the same visual object, different people usually describe it in various forms, as they focus on different aspects of object properties (*e.g.*, color, shape, texture, and relationship with surroundings). This diversity makes vision language (VL) alignment cumbersome, where a comprehensive set of language expressions should be collected for model training. Fortunately, emerging VLMs (Liu et al., 2023a; Ye et al., 2023; Zhang et al., 2023b; Sun et al., 2024; Yuan et al., 2024; You et al., 2024; Zhang et al., 2024) have recently been leveraged to produce human-like expressions. The auto-generation of language expressions for visual objects eases the difficulty of collecting training data pairs. By training LOD models with extensive VL data, studies (Pi et al., 2024; Dang et al., 2024; Kong et al., 2024) improve detection performance accordingly, especially when the language query is diverse to describe the target object.

The language expressions generated via VLMs, although aligned with human preference, may not accurately describe the target object due to model hallucinations. Fig. 1 shows two examples. A small object shown in Fig. 1(a) leads VLMs to generate erroneous expressions. Moreover, a general

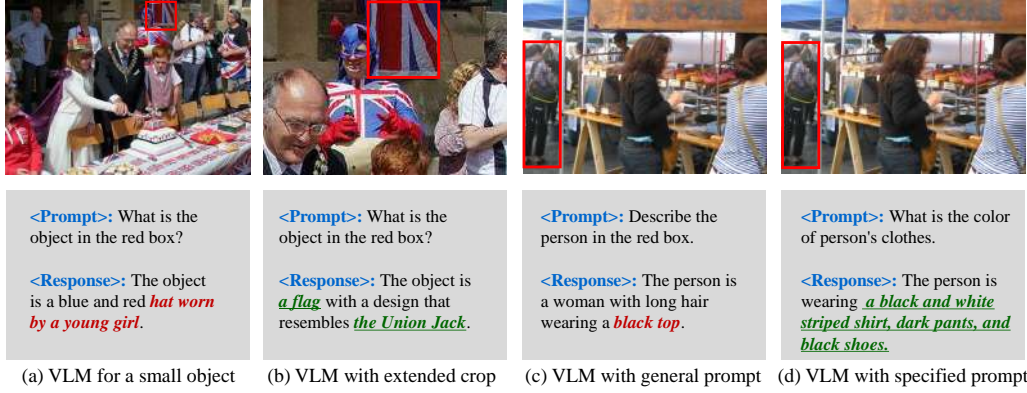


Figure 1: Examples of adaptive image and prompt modifications refine language expressions. For a small object in (a), VLM produces erroneous content marked in red. In (b), we crop the local region of (a) and obtain refined content marked in green. Another example is in (c), where a general prompt leads to erroneous content while a specific prompt in (d) does not.

text prompt without specifying the target object shown in Fig. 1(c) makes VLMs incorrectly describe visual content. For model hallucinations on small objects, we analyze that VLMs are trained via extensive image-caption pair data (Radford et al., 2021; Schuhmann et al., 2022), where the caption mainly depicts global image content rather than local objects. The ignorance of local object context in training data makes VLMs hallucinate small objects. On the other hand, text prompts without specifying the target object (e.g., ‘in a red box’) lead to incorrect detail descriptions from VLMs. A lack of object identity in the prompt makes VLMs insensitive to object details and expresses them erroneously. When incorporating these inaccurate language expressions, the alignment of object and language becomes fragile and impedes LOD performance improvement along with VL data scaling up.

In this work, we propose to re-align language expressions to visual objects automatically to refine VL data quality from the alignment perspective. Our re-alignment is conducted via a workflow (i.e., Real-LOD) controlled by an LLM-powered agent (i.e., Real-Agent).¹ Fig. 2 shows a glimpse of where there are three steps (i.e., planning, tool use, and reflection) to form a cycle. Given an input image with detected objects, we first convert this image into captions, which are sent into Real-LOD together with object location, category, and raw language expressions from the VLMs initially used. Then, our agent automatically reasons the current state and arranges further actions. The state/action represents our neural symbolic design in the workflow, where we have predefined five states indicating how language aligns with the visual objects. Each state is followed by an arranged action. After the planning step, our agent takes action to construct adaptive VL prompts for the tool models (i.e., VLM/LLM). The customized prompts enable tool models to either gather more visual observations or refine current expressions. After the tool use step, the refined expression is sent to an LLM-based reflector for feedback. The feedback is then provided to our agent for planning in the next cycle. Fig. 5 shows an example where the raw expression is gradually refined to align with the target object.

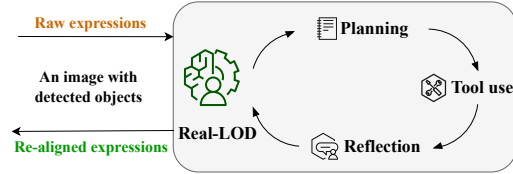


Figure 2: Glimpse of our Real-LOD. It takes image captions with detected objects and raw expressions as inputs. It gradually re-aligns expressions to match objects well. By using better-aligned training data pairs, we improve the performance of LOD.

Our Real-LOD refines language-object data pairs via re-alignment for LOD model training. Our Real-Model is a prevalent model structure with a Swin-B backbone (Liu et al., 2021). We train this

¹For presentation clarity, we refer to Real-LOD as our agentic workflow, Real-Agent as the LLM-powered agent, Real-Data as our constructed dataset, and Real-Model as our trained LOD model.

model using our constructed dataset **Real-Data** where there are 0.18M images that contain 1.4M language-object paired data. In the standard benchmarks (Schulter et al., 2023; Xie et al., 2023), we surpass existing methods by around 50%. This indicates that data quantity and quality are important for LOD training. In addition to the amount of image data that scales up, our Real-LOD can preserve the quality of the data pair. This potential directs a new trend that expanding high-quality paired data further improves LOD performance from a data-alignment perspective.

2 RELATED WORK

Language-based object detection. LOD requires models to locate the associated instances according to diverse expressions. Benefiting from visual-language detector development, the accuracy of LOD tasks is improved rapidly. MDETR (Kamath et al., 2021) first proposed an end-to-end modulated detector that detects objects by a given query. In GLIP (Li et al., 2022), it presents a language-image pre-train model for understanding object-level, category-aware visual representations. GDINO (Liu et al., 2023c) presented an open-set object detector within an effective fusion module that allows the detection of objects with textual inputs such as category names or referring expressions. FIBER (Dou et al., 2022) proposed a new visual-language model architecture that can handle different tasks such as visual question answering (VQA), image caption, object detection, and so on. APE (Shen et al., 2023b) proposed a universal visual perception model to align visual and language representation on broad data at once so that it is able to conduct different language-visual tasks without task-specific fine-tuning. OWL-V2 (Minderer et al., 2023) proposed an architecture without any fusion modules. They use 1B language-object pair data to align image and textual features directly. The above methods utilized language-object pair data to train their detectors, including COCO (Lin et al., 2014), Objects365 (Shao et al., 2019), OpenImage (Kuznetsova et al., 2020), SBU (Ordonez et al., 2011), GoldG (Li et al., 2022), CC (Sharma et al., 2018; Changpinyo et al., 2021; Xu et al., 2023), LVIS (Gupta et al., 2019), Flickr30K (Plummer et al., 2017), GRIT (Gupta et al., 2022), and V3Det (Wang et al., 2023a).

Agentic workflows. Intelligent agents empowered by LLMs are able to solve a wide range of complex tasks by following user’s instructions (Askell et al., 2021; Liu et al., 2023d; Significant Gravitass, 2023; Yohei Nakajima, 2023; Reworkd, 2023). Due to the strong understanding and reasoning abilities of LLM (Wei et al., 2022; Wang et al., 2023b), these agents are capable of making plans to achieve specified goals, mastering tools to execute tasks (Yao et al., 2023; Liu et al., 2023b; Tang et al., 2024; Yang et al., 2023a; Guo et al., 2024; Shen et al., 2023a; Cai et al., 2024), generating reflection to refine outputs (Madaan et al., 2023; Shinn et al., 2023; Yu et al., 2024; An et al., 2023; Gou et al., 2024), and even collaborating with other agents (Chen et al., 2023a; Xu et al., 2024; Holt et al., 2024). HuggingGPT (Shen et al., 2023a) is presented as a powerful agent that leverages LLM to connect various AI models for solving different tasks. This agent is designed to understand and dismantle given AI tasks, as well as plan and select appropriate AI models to execute each subtask automatically. Similarly, LLaVA-Plus (Liu et al., 2023b) maintains a skill repository that contains a wide range of vision-language tools to fulfil many real-world multi-modal tasks. Other examples include Gorilla (Patil et al., 2023), GPT4tools (Yang et al., 2023a), and ToolAlpaca (Guo et al., 2024), which are fine-tuned LLMs with the ability to utilize available APIs. Additionally, recent studies have also shed light on improving agent performance through train-free approaches. One of the main ideas is reflection, where agents provide feedback to themselves and use it to refine their outputs. Self-Refine (Madaan et al., 2023) and Reflexion (Shinn et al., 2023) are the typical examples to reinforce agents with linguistic feedback, while CRITIC (Gou et al., 2024) introduces external tools into the reflection process with a human-predefined execution logic which is relatively fixed. Different from previous works, Real-LOD pioneer designs an entire agentic workflow containing the above three steps to advance the alignment quality of VL data for LOD tasks.

3 RE-ALIGNING LANGUAGE TO VISUAL OBJECTS

In this section, we first revisit the LOD framework, showing how paired VL-inputs predict target objects in Sec. 3.1. Then, we illustrate the key steps of our Real-LOD (*i.e.*, planning, tool use, reflection) in Sec. 3.2. An example is provided in Fig. 5 to intuitively demonstrate how language expression is refined via our re-alignment scheme. The refined expressions constitute training data pairs to improve LOD performance.

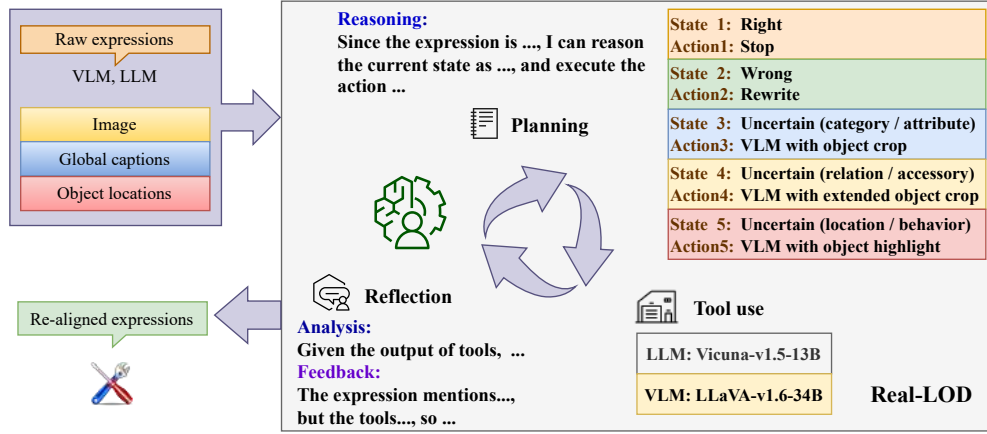


Figure 4: Overview of Agentic workflow. The inputs are images with captions, detected objects, and raw expressions from VLM and LLM. Our **Real-Agent** reasons the state and arranges the action. During action execution, our **Real-Agent** uses VLM and LLM to re-perceive visual content and refine expressions (*i.e.*, tool use). Then, the results are analyzed by an LLM for reflection. The feedback is provided to **Real-Agent** for planning in the next cycle.

3.1 LOD FRAMEWORK AND LANGUAGE EXPRESSION GENERATIONS

The language-based object detection (LOD) framework typically consists of two encoders, a few interaction modules, and a decoder. Fig. 3 shows an overview. The inputs of LOD are one image and language expressions formulated by words, phrases, or sentences. LOD uses image and text encoders to obtain their embeddings independently. Then, the expressions interact with visual objects to formulate a joint cross-modal feature space. These interactions are usually conducted via cross-attention operations. Afterwards, LOD introduces a decoder module to localize the corresponding object based on each expression. The training losses (*e.g.*, L1 loss, GIOU loss (Rezatofighi et al., 2019), contrastive loss (Li et al., 2022)) are typically from DETR-based methods (Carion et al., 2020; Kamath et al., 2021; Zhang et al., 2023a).

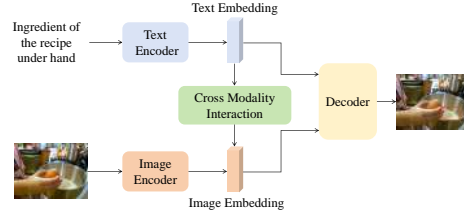


Figure 3: Overview of a general LOD framework. The paired VL-data are independently encoded and then interacted to decode results.

The LOD framework establishes the connection between language and objects. The training data contains images, object bounding boxes (bbxs), and language expressions. Previous datasets (Mao et al., 2016; Plummer et al., 2017; Krishna et al., 2017) tend to collect expressions from human participants, which constructs a limited amount of paired data and bottlenecks the detection performance. Recently, studies (Dang et al., 2024; Pi et al., 2024) have leveraged VLMs to generate human-like expressions for visual objects. The training data amount is extensively scaled up, and the learned LOD model captures diversified object descriptions. Following their spirit, we use a VLM model LLaVA-v1.6-34B (Liu et al., 2024) to generate 673k language expressions for 188k images with 336.5k objects. Also, we use an LLM Vicuna-v1.5-13B (Zheng et al., 2023) to expand the number of expressions from 673k to 1,346.1k by generating synonyms. The details of raw expression generation are presented in the Sec. A of the Appendix. After obtaining language-object paired data, we use SigLIP (Zhai et al., 2023) to calculate the VL matching score. For the paired data whose score is lower than 0.5, we use Real-LOD to re-align raw language expressions as illustrated in Sec. 3.2. This is because we leverage SigLIP to exclude 75% of training data from our workflow, leaving only 25% to be processed.

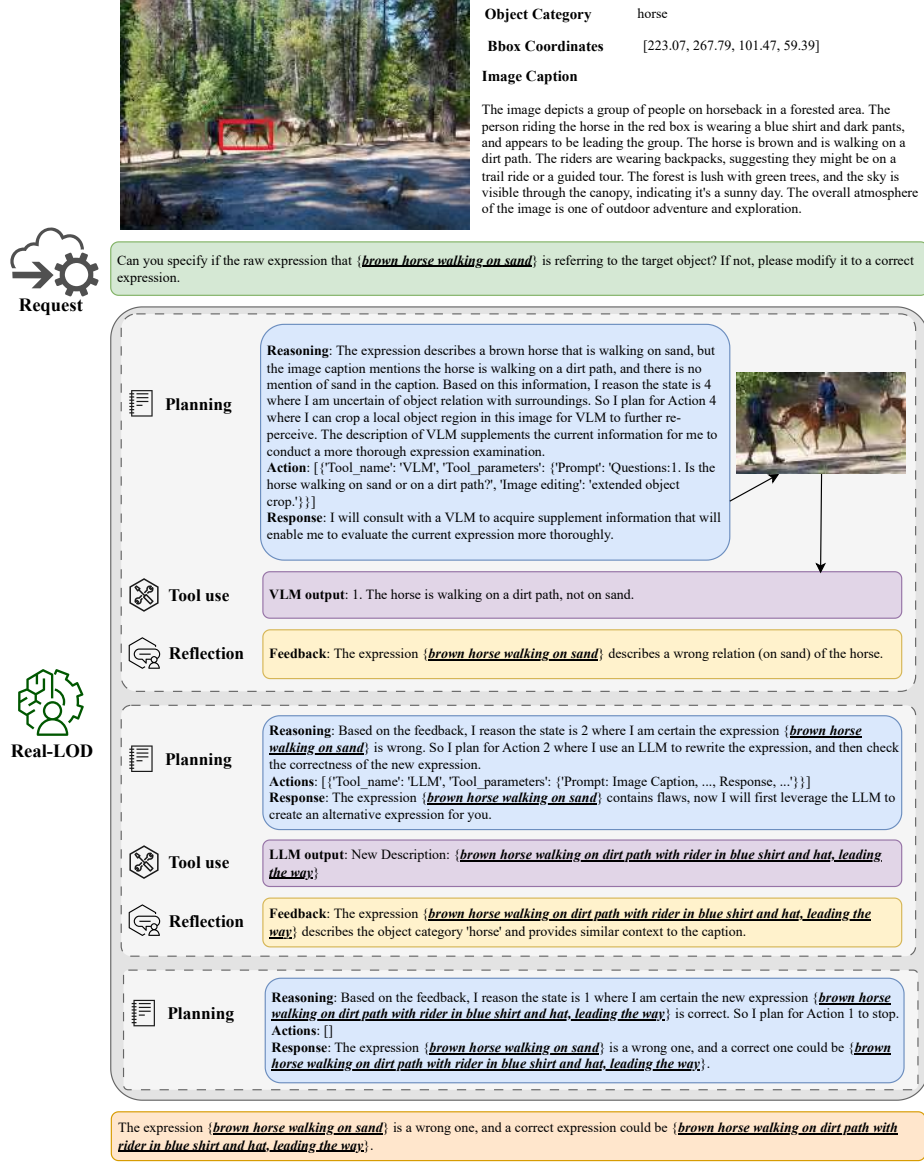


Figure 5: An example of how Real-LOD re-aligns one raw expression to given image. Based on the input image, caption, and detected objects, Real-LOD performs planning, tool use, and reflection in a cyclic workflow for state reasoning, action execution, and result feedback. The image and prompt are adaptively adjusted for tool models to supplement customized object descriptions, which benefit expression re-alignment.

3.2 AGENTIC WORKFLOWS FOR LANGUAGE EXPRESSION RE-ALIGNMENT

The generated language expressions may not match visual objects. As illustrated in Sec. 1, either local context ignorance or unspecific text prompts lead to model hallucination. To solve this problem, we design a cyclic workflow to enable VLM to adaptively focus on local regions and specify text prompts according to the target object. This workflow is controlled by our **Real-Agent**, which is fine-tuned from ChatGLM-6B (Zeng et al., 2023). Fig. 4 shows an overview. It consists of planning, tool use, and reflection steps to gradually refine raw expressions. To facilitate VL re-alignment, we have performed neural symbolic design in the planning and tool use steps where we predefined 5 states and actions, which are illustrated as follows.

Planning. In this step, we have predefined 5 states indicating how expressions are aligned to the target object from the view of VLM. Each state corresponds to one action to be executed. Formulating these states/actions is motivated via our data analysis in Sec. 3.3, where we observe how VL misalignment occurs in practice. Given the input, our **Real-Agent** reasons the current state and arranges action accordingly. To be specific, based on our finding that LLM reasons more accurately in pure language form than in VL form, we use an LLM as the **Real-Agent** with textual inputs, including given expression, image caption, object category, and reflector output from the last cycle (Empty if at first cycle). In addition, the five predefined states/actions are as follows:

State 1: Right. Action 1: Stop. **Real-Agent** is certain that the current language expression matches the target object. **Real-Agent** will stop the workflow and output the current expression.

State 2: Wrong. Action 2: Rewrite. **Real-Agent** is certain that the current expression does not match the target object. So **Real-Agent** will use an LLM to regenerate the expression. The in-context prompt will be generated following the template in Tab. 10 of the appendix for rewriting.

State 3: Uncertain (category/attribute). Action 3: VLM with object crop. **Real-Agent** is uncertain whether the current expression matches the target object. The uncertainty resides in the object category or attribute. So **Real-Agent** plans to crop the object region and use a VLM for further re-perception. The description from VLM will be kept in the text prompt for the next step.

State 4: Uncertain (relation/accessory). Action 4: VLM with extended object crop. Similar to State 3, **Real-Agent** is uncertain of object relation (with surroundings) or accessory. It plans to crop a larger region covering the target object and uses a VLM for re-perception. The description from VLM will be kept in the text prompt for the next step.

State 5: Uncertain (location/behavior). Action 5: VLM with object highlight. Similar to State 3, **Real-Agent** is uncertain of object location (in image) or behavior. It plans to highlight the object region using a red rectangle (Shtedritski et al., 2023) and uses a VLM for re-perception. The description from VLM will be kept in the text prompt.

When executing actions, we only refine language expressions in Action 2, while in Action 3,4,5, we use VLM to supplement descriptions as in-context prompts. These prompts will be utilized in the next cycle to facilitate state reasoning and action executions.

Tool use. In the planning step, **Real-Agent** has scheduled to use several tools (*i.e.*, VLM and LLM) when executing actions. We prepare a toolset in advance where there are one LLaVA-v1.6-34B model for VLM usage and one Vicuna-v1.5-13B model for LLM usage. Based on its reasoning about the state of the current expression, **Real-Agent** adaptively modulates visual content and text prompts by setting up "Prompt" and "Image editing" parameters for scheduled tools. Then, the tool can be used effectively to get desired responses from VLM to improve the expression refinement. For example, when executing VLMs for visual content re-perception, **Real-Agent** will edit the image via cropping or highlighting as planned according to the object region. Also, the customized text prompts designed by **Real-Agent** are more specifically related to the target object. In this way, **Real-LOD** can effectively reduce model hallucinations, improving language and object connections by re-aligning expressions. The text and visual prompts are shown in Tab. 12 of the appendix.

Reflection. After using tools, **Real-Agent** has finished action executions. We use an LLM (Vicuna-v1.5-13B) as a reflector to analyze the results by incorporating the image caption. It verifies whether the current expression matches the target object. For State 3-5, where **Real-Agent** is uncertain, the reflector helps **Real-Agent** be confident in judging whether the expression is correct or wrong. For State 2 where **Real-Agent** has planned to rewrite the expression, the reflector examines the correctness of the new expression. The analysis of the reflector will be formulated as feedback to **Real-Agent** to facilitate its planning in the next cycle.

3.3 DATA ANALYSIS OF LANGUAGE AND VISUAL OBJECTS

Training data for Real-Agent. We prepare training data in the text form to finetune **Real-Agent** (ChatGLM-6B). First, we randomly collect images with detected objects from Objects365 (Shao et al., 2019) datasets. Then, similar to Sec. 3.1, we use VLM to generate raw expressions and collect the data pairs that are filtered out by SigLIP, *i.e.*, the matching score is lower than 0.5. In total, we prepare 15k input data to train **Real-Agent**. Each input data contains the object category, raw

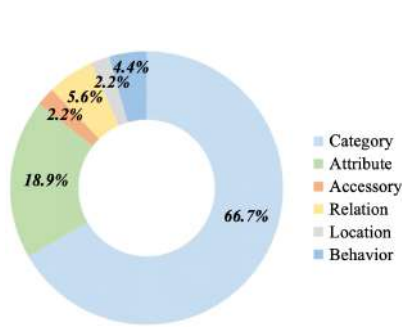


Figure 6: Percentage of 6 aspects for mismatch expressions where category and attribute consume the majority.

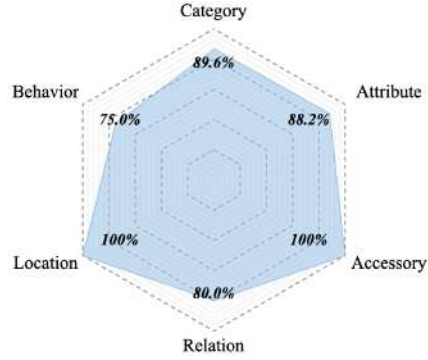


Figure 7: Success rate of expression re-alignment via Real-LOD in 6 aspects.

expression, and reasoning from the LLM-based reflector defined in Sec. 3.2 to examine whether the raw expression matches the target object. Then, we manually set the state for each input data by ourselves and collect responses (including "reasoning" and "actions") via an LLM (Vicuna-v1.5-13B) with text prompts including several hand-craft in-context examples in Tab. 11 following the spirit of LLaVA Liu et al. (2023a). Finally, a manual check is conducted to ensure no error in the fine-tuning data. The training process is conducted in a parameter-efficient form (*i.e.*, LoRA (Hu et al., 2021)) that does not affect the reasoning ability of ChatGLM-6B.

Analysis of language and visual objects.

Our Real-LOD corrects raw expressions filtered out via SigLIP. As we design actions for expression correction in advance, we analyze how these expressions mis-align to the target object. We randomly select three hundred filtered expressions and manually check each for a detailed observation.

Overall, we summarize the mis-alignment reasons in 6 aspects based on the observed expressions: 1) **Category** (the expression describes another object rather than the target one); 2) **Attribute** (the expression provides wrong attributes such as color, shape, and texture of the target object); 3) **Accessory** (incorrect accessory descriptions of the target object); 4) **Location** (wrong relative location of the target object in the image); 5) **Relation** (incorrect object relationship with surroundings); 6) **Behavior** (incorrect object/human behaviors). Fig. 8 shows representative examples of how expressions listed in each aspect will be corrected. These 6 aspects motivate our neural symbolic action designs in Sec. 3.2 where image editing operations ('object crop', 'extended object crop', and 'object highlight') are utilized for VLM to perceive object related contents further. Fig. 6 shows the percentage of these 6 aspects in our observed expressions where most of them reside in the category and attribute aspects. After refinement, we compute the success rate of expressions from each aspect as shown in Fig. 7, where major expressions from category and attribute aspects can be effectively refined.

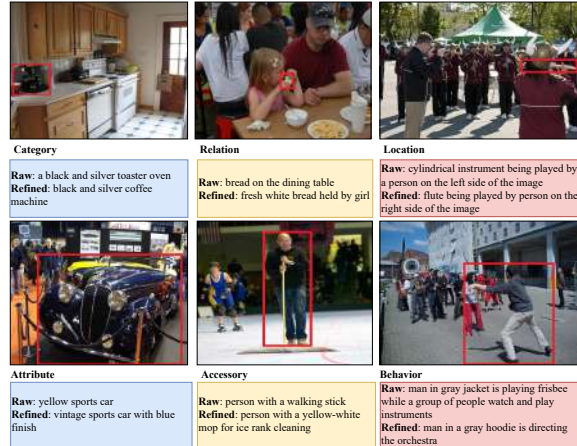


Figure 8: Example summary of misaligned raw expressions in 6 aspects, followed by our re-alignment.

Analytical experiment for Real-LOD. Besides summarizing 6 aspects of mismatched raw expressions, we analyze how effective our Real-LOD is for re-alignment. Although we have designed corresponding actions to enable VLM for a re-perception, the accurate state reasoning and action planning will determine the refinement quality. For the inputs listed in Fig. 4, **Real-Agent** shall reason accurately to identify which state they belong to and execute the action accordingly. To analyze the reasoning ability of Real-Agent, we sample 11k samples and introduce a scheme for comparison by replacing the planning step with a step where one of the states/actions is selected randomly for

further expression refinement. The reflector is used in both workflows to identify whether the final expression refinement is successful, and we set the maximum round to 3. After refining expressions using Real-LOD and the random selection, we find that the success rate ² is 74.7% v.s. 35.6%. This comparison shows that accurate reasoning from Real-Agent significantly improves expression correctness. Furthermore, we examine the matching score between image and expressions refined by these two refinement schemes via SigLIP. Our Real-Agent improves the average matching score by 66.27% (*i.e.*, from 0.0673 to 0.1119), while random selection improves by 32.69% (*i.e.*, from 0.0673 to 0.0893). This indicates Real-Agent improves the SigLIP matching score more than the random selection scheme (66.27% v.s. 32.69%). From the comparisons of re-alignment success rate and SigLIP score improvement, our Real-Agent demonstrates effectiveness in reasoning input state, planning action correctly, and successfully refining raw expressions. We also provide more analytical experiments in Sec. J.

4 EXPERIMENTS ON LANGUAGE-BASED OBJECT DETECTION

Real-Model is a prevalent LOD model structure illustrated in Sec. 3.1. We use the re-aligned data Real-Data to train this model. The training details are provided in the Sec. H.2 of the Appendix. In this section, we focus on evaluating our model in the LOD scenario. We illustrate benchmark datasets, ablation studies, evaluations of existing methods, and analysis of computational cost.

Standard benchmarks. The benchmarks we use for evaluation are Omnilabel (Schulter et al., 2023), DOD (Xie et al., 2023), RefCOCO/g/+ (*i.e.*, RefCOCO, RefCOCOg, RefCOCO+) (Yu et al., 2016; Mao et al., 2016) and OVDEval (Yao et al., 2024). Omnilabel is collected from three object detection datasets (*i.e.*, Objects365 (Shao et al., 2019), OpenImage (Kuznetsova et al., 2020), and COCO (Lin et al., 2014)). It is divided into these three subsets for evaluation. There are 12.2k images, 20.4k object bbxs, and 15.8k expressions. The evaluation metrics are AP, AP-des-pos, and AP-des-S/M/L, which measure the average precision of object descriptions from overall, only positive, and various length perspectives. DOD contains 1k images with 18k bbxs and 422 descriptions. It uses ‘Presence’ and ‘Absence’ to evaluate detection performance upon positive and negative queries. The RefCOCO/g/+ are from the COCO datasets with 9.9k images, 22.9k bbxs, and 46.5k descriptions. The details of OVDEval are shown in Sec. E. For all the benchmarks, we follow standard protocols to ensure a fair comparison.

Real-Data. Our Real-LOD naturally constructs a dataset via re-aligned language expressions. We randomly select images from Objects365 (Shao et al., 2019), OpenImage (Kuznetsova et al., 2020), and LVIS (Gupta et al., 2019) datasets with all categories covered. There are 188k images with 1,346.1k object-query pairs in total. Among them, 473.8k pairs are filtered out by SigLIP, with 307.1k being re-aligned. The final pairs for our Real-Model training are 1,179.4k. We name our dataset Real-Data.

4.1 COMPARISONS WITH STATE-OF-THE-ART LOD METHODS

We evaluate our Real-Model with existing LOD methods on the standard benchmarks, including Omnilabel, DOD, and RefCOCO/g/+ in Table 1-3. In each table, we list the vision backbones leveraged by LOD methods, source of training images (*i.e.*, ‘Source’), and the number of images used for training (*i.e.*, ‘#Img’). We use VG, OI, O365, RefC/g/+, and CC to denote Visual Genome (Krishna et al., 2017), OpenImage (Kuznetsova et al., 2020), Objects365 (Shao et al., 2019), RefCOCO/g/+ (Yu et al., 2016), and Conceptual Captions (Sharma et al., 2018; Changpinyo et al., 2021; Xu et al., 2023), respectively. Besides, the detailed training image sources for each method can be found in Tab. 15.

In the Omnilabel benchmark, our Real-Model significantly outperforms existing LOD methods on all test sets. Especially on the OI set, under the AP-des metric, Real-Model surpasses the second-best mm-GDINO by a large margin (*i.e.*, 40.5% v.s. 23.2%). Meanwhile, under the AP-des-pos metric, Real-Model surpasses the same second-best mm-GDINO significantly (*i.e.*, 51.4% v.s. 34.5%). The superior performance of Real-Model is due to the high-quality language-object paired data provided

²Suppose N and N_s represent the number of total expressions and correctly refined expressions, respectively. The success rate can be formulated as $\frac{N_s}{N}$.

Table 1: State-of-the-art comparisons on the Omnilabel benchmark.

Subset	LOD method	Backbone	Source	#Img	AP-des	AP-des-pos	AP-des-S	AP-des-M	AP-des-L
COCO	MDETR (Kamath et al., 2021)	ENB3	COCO, VG, Flickr30K	0.3M	13.2	31.6	15.4	13.5	12.4
	GLIP (Li et al., 2022)	Swin-L	O365, OI, RefC/g/+, etc	17.5M	13.9	36.8	28.9	12.9	11.5
	mm-GDINO (Zhao et al., 2024)	Swin-B	GoldG, O365, COCO, etc	12M	15.2	47.0	29.3	14.9	15.1
	FIBER (Dou et al., 2022)	Swin-B	COCO, CC3M, SBU, etc	4M	14.3	38.8	31.3	12.7	16.1
	Real-Model	Swin-B	Real-Data	0.18M	26.2	59.7	39.4	25.4	24.3
O365	MDETR (Kamath et al., 2021)	ENB3	COCO, VG, Flickr30K	0.3M	3.2	5.9	3.0	3.2	2.7
	GLIP (Li et al., 2022)	Swin-L	O365, OI, RefC/g/+, etc	17.5M	24.0	35.2	44.5	20.5	11.8
	mm-GDINO (Zhao et al., 2024)	Swin-B	GoldG, O365, COCO, etc	12M	19.6	31.0	32.3	17.8	12.4
	FIBER (Dou et al., 2022)	Swin-B	COCO, CC3M, SBU, etc	4M	25.9	38.2	44.7	22.5	14.1
	Real-Model	Swin-B	Real-Data	0.18M	36.0	52.1	55.7	32.3	23.7
OI	MDETR (Kamath et al., 2021)	ENB3	COCO, VG, Flickr30K	0.3M	6.1	10.6	9.6	5.7	4.1
	GLIP (Li et al., 2022)	Swin-L	O365, OI, RefC/g/+, etc	17.5M	20.1	31.2	33.3	18.7	10.3
	mm-GDINO (Zhao et al., 2024)	Swin-B	GoldG, O365, COCO, etc	12M	23.2	34.5	32.3	23.8	16.9
	FIBER (Dou et al., 2022)	Swin-B	COCO, CC3M, SBU, etc	4M	20.1	30.9	34.1	18.5	10.5
	Real-Model	Swin-B	Real-Data	0.18M	40.5	51.4	54.9	37.8	30.6
ALL	MDETR (Kamath et al., 2021)	ENB3	COCO, VG, Flickr30K	0.3M	4.7	9.1	6.4	4.6	4.0
	GLIP (Li et al., 2022)	Swin-L	O365, OI, RefC/g/+, etc	17.5M	21.2	33.2	37.7	18.9	10.8
	mm-GDINO (Zhao et al., 2024)	Swin-B	GoldG, O365, COCO, etc	12M	20.8	33.1	31.9	19.8	14.1
	FIBER (Dou et al., 2022)	Swin-B	COCO, CC3M, SBU, etc	4M	22.3	34.8	38.6	19.5	12.4
	Real-Model	Swin-B	Real-Data	0.18M	36.5	52.1	54.4	33.2	25.5

Table 2: Evaluation results on the DOD benchmark.

LOD method	Backbone	Source	#Img	Full	Presence	Absence
OWL-V2 (Minderer et al., 2023)	ViT-L	WebLI	10B	9.6	10.7	6.4
UNINEXT (Yan et al., 2023)	ViT-H	O365, RefC/g/+	0.7M	20.0	20.6	18.1
GDINO (Liu et al., 2023c)	Swin-B	CC4M, O365, RefC/g/+, etc	5.8M	20.1	20.7	22.5
mm-GDINO (Zhao et al., 2024)	Swin-B	GoldG, O365, COCO, etc	12M	24.2	23.9	25.9
OFA-DOD (Xie et al., 2023)	RN101	CC12M, SBU, VG, etc	16M	21.6	23.7	15.4
APE-B (Shen et al., 2023b)	ViT-L	LVIS, O365, RefC/g/+, etc	2.6M	30.0	29.9	30.3
Real-Model	Swin-B	Real-Data	0.18M	34.1	34.4	33.2

by **Real-Data**. On the other hand, we observe that the training data size used for GLIP is larger than **Real-Model**, but the accuracy is around 50% of ours. This indicates that data quality is as important as data quantity to achieve superior results.

Tables 2-3 shows the evaluation results on DOD and RefCOCO/g/+ benchmarks, respectively. The results are similar to those in the Omnilabel benchmark. Using a small amount of training data, our **Real-Model** achieves favourable results under various metrics, which surpasses existing LOD methods. This performance gain is due to our **Real-Data** data pairs, where diversified language expressions improve the generalizations of language and object alignment. As a result, our **Real-Data** datasets, with the same images and objects but diversified language descriptions, benefit **Real-Model** in achieving state-of-the-art performance.

4.2 ABLATION STUDY

We train our **Real-Model** by using three training data pair configurations (*i.e.*, A, B, and C forms) and evaluate the corresponding LOD performance on the Omnilabel benchmark. We randomly select 94k images from Objects365 (O365) and OpenImage (OI) datasets covering all categories, which is a subset of **Real-Data**. These images, together with target objects and raw expressions, constitute our original training data pairs with an amount of 933k (*i.e.*, A form). Moreover, we use SigLIP to filter out some data pairs where expressions do not match the target object. The remaining pairs are 695k (*i.e.*, B form). Furthermore, we use Real-LOD to re-align mismatched pairs to add them back to B, which increases the number of pairs to 863k (*i.e.*, C form). We use data pairs in A, B, and C forms to train **Real-Model** separately and evaluate the corresponding performance. This helps analyze how our Real-LOD improves LOD from a data-alignment perspective.

Tab.4 shows the LOD results via three data configurations (*i.e.*, A, B, and C forms). It demonstrates that on the COCO test set, **Real-Model** achieves a 21.2% AP by using all the training data pairs (*i.e.*, A form). After removing data pairs with mismatched expressions, **Real-Model** increases to 22.2% (*i.e.*, B form). This improvement indicates that data quality essentially benefits LOD performance.

Table 3: Evaluation results on the RefCOCO/g/+ benchmark. ‘*’ indicates that the model employs RefCOCO/g/+ for training.

LOD method	Backbone	Source	#Img	RefCOCO			RefCOCO+			RefCOCOg	
				val	testA	testB	val	testA	testB	val-u	test-u
MDETR (Kamath et al., 2021)	ENB3	COCO, VG, Flickr30K	0.3M	73.4	-	-	58.8	-	-	57.1	-
APE-A (Shen et al., 2023b)	ViT-L	COCO, LVIS, O365, etc	2.0M	34.2	34.8	36.1	33.5	32.3	36.0	38.9	40.5
Real-Model	Swin-B	Real-Data	0.18M	74.0	79.6	66.0	76.4	83.1	68.5	80.8	81.2
GLIP* (Li et al., 2022)	Swin-L	O365, OI, RefC/g/+, etc	17.5M	53.1	59.4	46.8	54.0	59.4	47.0	60.7	60.4
GDINO* (Liu et al., 2023c)	Swin-B	CC4M, O365, RefC/g/+, etc	5.8M	-	-	-	73.6	82.1	64.1	78.3	78.1
APE-B* (Shen et al., 2023b)	ViT-L	LVIS, O365, RefC/g/+, etc	2.6M	84.6	89.2	80.9	76.4	82.4	66.5	80.0	80.1
Real-Model*	Swin-B	RefC/g/+, Real-Data	0.24M	91.3	93.1	88.0	85.4	90.3	78.6	88.4	89.0

Table 4: Ablation study on Omnilabel benchmark. Our training data pairs consist of images, target objects, and expressions (expr). We adjust training data pairs by processing raw expr differently (*i.e.*, SigLIP filter and Real-LOD) and evaluate the corresponding performance. Note that we use a subset of **Real-Data**.

Test subset	Training data type	#Img	AP-des	AP-des-pos	AP-des-S	AP-des-M	AP-des-L
COCO	raw expr (A)	933k	21.2	59.4	31.3	21.1	18.6
	raw expr w.filter (B)	695k	22.2	59.4	32.4	21.9	19.4
	raw expr w.filter + Real-LOD (C)	863k	24.2	59.6	35.2	24.2	21.1
O365	raw expr (A)	933k	27.6	43.1	39.8	25.5	17.9
	raw expr w.filter (B)	695k	28.5	43.7	40.9	26.2	18.5
	raw expr w.filter + Real-LOD (C)	863k	32.4	48.5	47.5	30.0	21.3
OI	raw expr (A)	933k	30.5	43.0	37.2	30.3	23.2
	raw expr w.filter (B)	695k	31.4	43.5	38.1	31.2	24.0
	raw expr w.filter + Real-LOD (C)	863k	33.5	44.9	42.2	32.9	24.8

Then, our Real-LOD refines filtered data pairs for a supplement, which improves **Real-Model** to 24.2% (*i.e.*, C form). It shows that Real-LOD increases data quantity with high quality, leading to further LOD improvement. The results on the other two test sets (*i.e.*, O365 and OI) indicate similar phenomena. When training **Real-Model**, data quality also has a influential impact on LOD performance, especially when the data quantity is increasing. Our Real-LOD re-aligns mismatched object and language pairs to increase data quantity while preserving data quality. To this end, our **Real-Model** learned with re-aligned data in C form performs best on the Omnilabel benchmark.

4.3 ANALYSIS ON COMPUTATIONAL COST

In our Real-LOD, we also leverage two strategies to further mitigate workflow time costs: 1) We leverage SigLIP to exclude 75% of training data from our workflow, leaving only 25% to be processed. 2) We set the max cycle number of our workflow as 4 to trade off time cost and performance. We elaborate on our computation cost in Tab. 14. For refining one expression, we report the average number of calls for each step and the time cost during each call. The time cost is reported based on 48 V100 32G GPUs for our workflow execution. For refining one expression, our workflow takes 1.579 seconds in total, with an average cycle number of 3.08. We also provide the distribution of iteration numbers in Fig. 18. Note that the max iteration number here is 10 for investigation. In addition, our workflow is completely offline without bringing additional computational burden to LOD model inference.

5 CONCLUSIONS

Re-aligning language to visual objects has been developed from manual descriptions to automatic VLM generations. The data pairs are scaling up to advance the connection performance via LOD. The generated descriptions may not match the objects due to model hallucinations. We thus propose Real-LOD to refine the language expressions gradually via agentic workflows. The data quality is preserved along with the increased data quantity. We train a prevalent LOD model using our data to largely surpass existing LOD methods. Our automatic workflow contains the expanding potential to re-align language descriptions of any objects. With an open vocabulary detector to locate objects with short category labels and VLMs to expand expression, our Real-LOD will continuously produce high-quality training pairs to scale up LOD performance.

ETHICAL STATEMENT

We declare that our research does not present any potential ethical issues. The study does not involve human subjects, sensitive data, or methodologies that could result in harmful outcomes or biases. All data this work uses is publicly available, and no privacy or security concerns are implicated.

REPRODUCIBILITY STATEMENT

Transparency and reliability are crucial to our research. In this statement, we summarise the measures taken to facilitate the reproducibility of our work and provide references to the relevant contents in the main paper and appendix.

Source code. We intend to make our source code, model weights, and datasets available to the public following the paper’s acceptance. It will allow the following researchers to access and utilize our code to reproduce our experiments and results. The detailed installation and execution instructions will be listed in ‘README.md.’

Experimental setup. We provide the basic implementation information of our Real-LOD in Sec. 3.1 and Sec. 3.2. Besides, we provide the experimental setup and evaluation settings in Sec. 4 and Sec. H.3. The details of Real-Data are listed in the Sec. 3.3 and Sec. 4. Moreover, the training and architectural details of Real-Model can be found in the Sec. H.2 and Sec. H.4 of the Appendix.

We provide the above resources and references to ensure the reproducibility of our work. It enables fellow researchers to verify our method. We also welcome any inquiries or requests for further clarification on our methods.

REFERENCES

- Hassan Akbari, Svebor Karaman, Surabhi Bhargava, Brian Chen, Carl Vondrick, and Shih-Fu Chang. Multi-level multimodal common semantic space for image-phrasе grounding. In *IEEE/CVF Conference on Computer Vision and Pattern Recognition*, 2019.
- Shengnan An, Zexiong Ma, Zeqi Lin, Nanning Zheng, Jian-Guang Lou, and Weizhu Chen. Learning from mistakes makes llm better reasoner. *arXiv preprint arXiv:2310.20689*, 2023.
- Amanda Askell, Yuntao Bai, Anna Chen, Dawn Drain, Deep Ganguli, Tom Henighan, Andy Jones, Nicholas Joseph, Ben Mann, Nova DasSarma, et al. A general language assistant as a laboratory for alignment. *arXiv preprint arXiv:2112.00861*, 2021.
- Tianle Cai, Xuezhi Wang, Tengyu Ma, Xinyun Chen, and Denny Zhou. Large language models as tool makers. In *International Conference on Learning Representations*, 2024.
- Nicolas Carion, Francisco Massa, Gabriel Synnaeve, Nicolas Usunier, Alexander Kirillov, and Sergey Zagoruyko. End-to-end object detection with transformers. In *European Conference on Computer Vision*, 2020.
- Soravit Changpinyo, Piyush Sharma, Nan Ding, and Radu Soricut. Conceptual 12M: Pushing web-scale image-text pre-training to recognize long-tail visual concepts. In *IEEE/CVF Conference on Computer Vision and Pattern Recognition*, 2021.
- Kai Chen, Jiaqi Wang, Jiangmiao Pang, Yuhang Cao, Yu Xiong, Xiaoxiao Li, Shuyang Sun, Wansen Feng, Ziwei Liu, Jiarui Xu, Zheng Zhang, Dazhi Cheng, Chenchen Zhu, Tianheng Cheng, Qijie Zhao, Buyu Li, Xin Lu, Rui Zhu, Yue Wu, Jifeng Dai, Jingdong Wang, Jianping Shi, Wanli Ouyang, Chen Change Loy, and Dahua Lin. MMDetection: Open mmlab detection toolbox and benchmark. *arXiv preprint arXiv:1906.07155*, 2019.
- Weize Chen, Yusheng Su, Jingwei Zuo, Cheng Yang, Chenfei Yuan, Chen Qian, Chi-Min Chan, Yujia Qin, Yaxi Lu, Ruobing Xie, et al. Agentverse: Facilitating multi-agent collaboration and exploring emergent behaviors in agents. *arXiv preprint arXiv:2308.10848*, 2023a.
- Yixin Chen, Sai Kumar Dwivedi, Michael J Black, and Dimitrios Tzionas. Detecting human-object contact in images. In *IEEE/CVF Conference on Computer Vision and Pattern Recognition*, 2023b.

- Ronghao Dang, Jiangyan Feng, Haodong Zhang, Chongjian Ge, Lin Song, Lijun Gong, Chengju Liu, Qijun Chen, Feng Zhu, Rui Zhao, et al. Instructdet: Diversifying referring object detection with generalized instructions. In *International Conference on Learning Representations*, 2024.
- Zi-Yi Dou, Aishwarya Kamath, Zhe Gan, Pengchuan Zhang, Jianfeng Wang, Linjie Li, Zicheng Liu, Ce Liu, Yann LeCun, Nanyun Peng, et al. Coarse-to-fine vision-language pre-training with fusion in the backbone. In *Advances in Neural Information Processing Systems*, 2022.
- Shangqian Gao, Burak Uzkent, Yilin Shen, Heng Huang, and Hongxia Jin. Learning to jointly share and prune weights for grounding based vision and language models. In *International Conference on Learning Representations*, 2023.
- Zhibin Gou, Zhihong Shao, Yeyun Gong, yelong shen, Yujiu Yang, Nan Duan, and Weizhu Chen. CRITIC: Large language models can self-correct with tool-interactive critiquing. In *International Conference on Learning Representations*, 2024.
- Zhicheng Guo, Sijie Cheng, Hao Wang, Shihao Liang, Yujia Qin, Peng Li, Zhiyuan Liu, Maosong Sun, and Yang Liu. Stabletoolbench: Towards stable large-scale benchmarking on tool learning of large language models. In *International Conference on Learning Representations*, 2024.
- Agrim Gupta, Piotr Dollar, and Ross Girshick. Lvis: A dataset for large vocabulary instance segmentation. In *IEEE/CVF Conference on Computer Vision and Pattern Recognition*, 2019.
- Tanmay Gupta, Ryan Marten, Aniruddha Kembhavi, and Derek Hoiem. Grit: General robust image task benchmark. *arXiv preprint arXiv:2204.13653*, 2022.
- Samuel Holt, Max Ruiz Luyten, and Mihaela van der Schaar. L2MAC: Large language model automatic computer for extensive code generation. In *International Conference on Learning Representations*, 2024. URL <https://openreview.net/forum?id=EhrzQwsV4K>.
- Edward J Hu, Yelong Shen, Phillip Wallis, Zeyuan Allen-Zhu, Yanzhi Li, Shean Wang, Lu Wang, and Weizhu Chen. Lora: Low-rank adaptation of large language models. *arXiv preprint arXiv:2106.09685*, 2021.
- Aishwarya Kamath, Mannat Singh, Yann LeCun, Gabriel Synnaeve, Ishan Misra, and Nicolas Carion. Mdetrmmodulated detection for end-to-end multi-modal understanding. In *IEEE/CVF International Conference on Computer Vision*, 2021.
- Diederik P. Kingma and Jimmy Ba. Adam: A method for stochastic optimization, 2017.
- Fanjie Kong, Yanbei Chen, Jiarui Cai, and Davide Modolo. Hyperbolic learning with synthetic captions for open-world detection. *arXiv preprint arXiv:2404.05016*, 2024.
- Ranjay Krishna, Yuke Zhu, Oliver Groth, Justin Johnson, Kenji Hata, Joshua Kravitz, Stephanie Chen, Yannis Kalantidis, Li-Jia Li, David A Shamma, et al. Visual genome: Connecting language and vision using crowdsourced dense image annotations. *International Journal of Computer Vision*, 2017.
- Alina Kuznetsova, Hassan Rom, Neil Alldrin, Jasper Uijlings, Ivan Krasin, Jordi Pont-Tuset, Shahab Kamali, Stefan Popov, Matteo Mallocci, Alexander Kolesnikov, et al. The open images dataset v4: Unified image classification, object detection, and visual relationship detection at scale. *International Journal of Computer Vision*, 2020.
- Liunian Li, Pengchuan Zhang, Haotian Zhang, Jianwei Yang, Chunyuan Li, Yiwu Zhong, Lijuan Wang, Lu Yuan, Lei Zhang, and Jenq-Neng Hwang. Grounded language-image pre-training. In *IEEE/CVF Conference on Computer Vision and Pattern Recognition*, 2022.
- Tsung-Yi Lin, Michael Maire, Serge Belongie, James Hays, Pietro Perona, Deva Ramanan, Piotr Dollár, and C Lawrence Zitnick. Microsoft coco: Common objects in context. In *European Conference on Computer Vision*, 2014.
- Haotian Liu, Chunyuan Li, Qingyang Wu, and Yong Jae Lee. Visual instruction tuning. In *Advances in Neural Information Processing Systems*, 2023a.

- Haotian Liu, Chunyuan Li, Yuheng Li, Bo Li, Yuanhan Zhang, Sheng Shen, and Yong Jae Lee. Llava-next: Improved reasoning, ocr, and world knowledge, 2024. URL <https://llava-vl.github.io/blog/2024-01-30-llava-next/>.
- Shilong Liu, Hao Cheng, Haotian Liu, Hao Zhang, Feng Li, Tianhe Ren, Xueyan Zou, Jianwei Yang, Hang Su, Jun Zhu, Lei Zhang, Jianfeng Gao, and Chunyuan Li. Llava-plus: Learning to use tools for creating multimodal agents. *arXiv preprint arXiv:2311.05437*, 2023b.
- Shilong Liu, Zhaoyang Zeng, Tianhe Ren, Feng Li, Hao Zhang, Jie Yang, Chunyuan Li, Jianwei Yang, Hang Su, Jun Zhu, et al. Grounding dino: Marrying dino with grounded pre-training for open-set object detection. *arXiv preprint arXiv:2303.05499*, 2023c.
- Xiao Liu, Hao Yu, Hanchen Zhang, Yifan Xu, Xuanyu Lei, Hanyu Lai, Yu Gu, Hangliang Ding, Kaiwen Men, Kejuan Yang, et al. Agentbench: Evaluating llms as agents. *arXiv preprint arXiv:2308.03688*, 2023d.
- Ze Liu, Yutong Lin, Yue Cao, Han Hu, Yixuan Wei, Zheng Zhang, Stephen Lin, and Baining Guo. Swin transformer: Hierarchical vision transformer using shifted windows. In *IEEE/CVF International Conference on Computer Vision*, 2021.
- Aman Madaan, Niket Tandon, Prakhar Gupta, Skyler Hallinan, Luyu Gao, Sarah Wiegrefe, Uri Alon, Nouha Dziri, Shrimai Prabhumoye, Yiming Yang, et al. Self-refine: Iterative refinement with self-feedback. In *Advances in Neural Information Processing Systems*, 2023.
- Junhua Mao, Jonathan Huang, Alexander Toshev, Oana Camburu, Alan Yuille, and Kevin Murphy. Generation and comprehension of unambiguous object descriptions. In *IEEE/CVF Conference on Computer Vision and Pattern Recognition*, 2016.
- Matthias Minderer, Alexey Gritsenko, and Neil Houlsby. Scaling open-vocabulary object detection. In *Advances in Neural Information Processing Systems*, 2023.
- Vicente Ordonez, Girish Kulkarni, and Tamara Berg. Im2text: Describing images using 1 million captioned photographs. *Advances in Neural Information Processing Systems*, 2011.
- Adam Paszke, Sam Gross, Francisco Massa, Adam Lerer, James Bradbury, Gregory Chanan, Trevor Killeen, Zeming Lin, Natalia Gimelshein, Luca Antiga, Alban Desmaison, Andreas Köpf, Edward Yang, Zach DeVito, Martin Raison, Alykhan Tejani, Sasank Chilamkurthy, Benoit Steiner, Lu Fang, Junjie Bai, and Soumith Chintala. Pytorch: An imperative style, high-performance deep learning library, 2019.
- Shishir G. Patil, Tianjun Zhang, Xin Wang, and Joseph E. Gonzalez. Gorilla: Large language model connected with massive apis. *arXiv preprint arXiv: 2305.15334*, 2023.
- Renjie Pi, Lewei Yao, Jianhua Han, Xiaodan Liang, Wei Zhang, and Hang Xu. Ins-detclip: Aligning detection model to follow human-language instruction. In *International Conference on Learning Representations*, 2024.
- Bryan A. Plummer, Liwei Wang, Chris M. Cervantes, Juan C. Caicedo, Julia Hockenmaier, and Svetlana Lazebnik. Flickr30k entities: Collecting region-to-phrase correspondences for richer image-to-sentence models. *International Journal of Computer Vision*, 2017.
- Alec Radford, Jong Wook Kim, Chris Hallacy, Aditya Ramesh, Gabriel Goh, Sandhini Agarwal, Girish Sastry, Amanda Askell, Pamela Mishkin, Jack Clark, Gretchen Krueger, and Ilya Sutskever. Learning transferable visual models from natural language supervision. In *International Conference on Machine Learning*, 2021.
- Joseph Redmon, Santosh Divvala, Ross Girshick, and Ali Farhadi. You only look once: Unified, real-time object detection. In *IEEE/CVF Conference on Computer Vision and Pattern Recognition*, 2016.
- Shaoqing Ren, Kaiming He, Ross Girshick, and Jian Sun. Faster r-cnn: Towards real-time object detection with region proposal networks. In *Advances in Neural Information Processing Systems*, 2016.

- Reworkd. AgentGPT, 2023. URL <https://github.com/reworkd/AgentGPT>.
- Hamid Rezatofighi, Nathan Tsoi, JunYoung Gwak, Amir Sadeghian, Ian Reid, and Silvio Savarese. Generalized intersection over union: A metric and a loss for bounding box regression. In *IEEE/CVF Conference on Computer Vision and Pattern Recognition*, 2019.
- Christoph Schuhmann, Romain Beaumont, Richard Vencu, Cade Gordon, Ross Wightman, Mehdi Cherti, Theo Coombes, Aarush Katta, Clayton Mullis, Mitchell Wortsman, Patrick Schramowski, Srivatsa Kundurthy, Katherine Crowson, Ludwig Schmidt, Robert Kaczmarczyk, and Jenia Jitsev. Laion-5b: An open large-scale dataset for training next generation image-text models. In *Advances in Neural Information Processing Systems*, 2022.
- Samuel Schuster, Yumin Suh, Konstantinos M Dafnis, Zhixing Zhang, Shiyu Zhao, Dimitris Metaxas, et al. Omnilabel: A challenging benchmark for language-based object detection. In *IEEE/CVF International Conference on Computer Vision*, 2023.
- Shuai Shao, Zeming Li, Tianyuan Zhang, Chao Peng, Gang Yu, Xiangyu Zhang, Jing Li, and Jian Sun. Objects365: A large-scale, high-quality dataset for object detection. In *IEEE/CVF International Conference on Computer Vision*, 2019.
- Piyush Sharma, Nan Ding, Sebastian Goodman, and Radu Soricut. Conceptual captions: A cleaned, hypernymed, image alt-text dataset for automatic image captioning. In *Annual Meeting of the Association for Computational Linguistics*, 2018.
- Yongliang Shen, Kaitao Song, Xu Tan, Dongsheng Li, Weiming Lu, and Yueting Zhuang. Hugginggpt: Solving ai tasks with chatgpt and its friends in hugging face. In *Advances in Neural Information Processing Systems*, 2023a.
- Yunhang Shen, Chaoyou Fu, Peixian Chen, Mengdan Zhang, Ke Li, Xing Sun, Yunsheng Wu, Shaohui Lin, and Rongrong Ji. Aligning and prompting everything all at once for universal visual perception. *arXiv preprint arXiv:2312.02153*, 2023b.
- Noah Shinn, Federico Cassano, Ashwin Gopinath, Karthik Narasimhan, and Shunyu Yao. Reflexion: Language agents with verbal reinforcement learning. In *Advances in Neural Information Processing Systems*, 2023.
- Aleksandar Shtedritski, Christian Rupprecht, and Andrea Vedaldi. What does clip know about a red circle? visual prompt engineering for vlms. In *IEEE/CVF International Conference on Computer Vision*, 2023.
- Significant Gravitas. AutoGPT, 2023. URL <https://github.com/Significant-Gravitas/AutoGPT>.
- Weijie Su, Xizhou Zhu, Yue Cao, Bin Li, Lewei Lu, Furu Wei, and Jifeng Dai. Vi-bert: Pre-training of generic visual-linguistic representations. In *International Conference on Learning Representations*, 2020.
- Zeyi Sun, Ye Fang, Tong Wu, Pan Zhang, Yuhang Zang, Shu Kong, Yuanjun Xiong, Dahua Lin, and Jiaqi Wang. Alpha-clip: A clip model focusing on wherever you want. In *IEEE/CVF Conference on Computer Vision and Pattern Recognition*, 2024.
- Qiaoyu Tang, Ziliang Deng, Hongyu Lin, Xianpei Han, Qiao Liang, Boxi Cao, and Le Sun. Toolalpaca: Generalized tool learning for language models with 3000 simulated cases. *arXiv preprint arXiv:2306.05301*, 2024.
- Jiaqi Wang, Pan Zhang, Tao Chu, Yuhang Cao, Yujie Zhou, Tong Wu, Bin Wang, Conghui He, and Dahua Lin. V3det: Vast vocabulary visual detection dataset. In *IEEE/CVF International Conference on Computer Vision*, October 2023a.
- Xuezhi Wang, Jason Wei, Dale Schuurmans, Quoc V Le, Ed H. Chi, Sharan Narang, Aakanksha Chowdhery, and Denny Zhou. Self-consistency improves chain of thought reasoning in language models. In *International Conference on Learning Representations*, 2023b.

- Jason Wei, Xuezhi Wang, Dale Schuurmans, Maarten Bosma, Fei Xia, Ed Chi, Quoc V Le, Denny Zhou, et al. Chain-of-thought prompting elicits reasoning in large language models. In *Advances in Neural Information Processing Systems*, 2022.
- Chi Xie, Zhao Zhang, Yixuan Wu, Feng Zhu, Rui Zhao, and Shuang Liang. Described object detection: Liberating object detection with flexible expressions. In *Advances in Neural Information Processing Systems*, 2023.
- Jilan Xu, Junlin Hou, Yuejie Zhang, Rui Feng, Yi Wang, Yu Qiao, and Weidi Xie. Learning open-vocabulary semantic segmentation models from natural language supervision. In *IEEE/CVF Conference on Computer Vision and Pattern Recognition*, 2023.
- Peng Xu, Haoran Wang, Chuang Wang, and Xu Liu. Caca agent: Capability collaboration based ai agent. *arXiv preprint arXiv:2403.15137*, 2024.
- Bin Yan, Yi Jiang, Jiannan Wu, Dong Wang, Ping Luo, Zehuan Yuan, and Huchuan Lu. Universal instance perception as object discovery and retrieval. In *IEEE/CVF Conference on Computer Vision and Pattern Recognition*, 2023.
- Rui Yang, Lin Song, Yanwei Li, Sijie Zhao, Yixiao Ge, Xiu Li, and Ying Shan. Gpt4tools: Teaching llm to use tools via self-instruction. In *Advances in Neural Information Processing Systems*, 2023a.
- Zhengyuan Yang, Linjie Li, Jianfeng Wang, Kevin Lin, Ehsan Azarnasab, Faisal Ahmed, Zicheng Liu, Ce Liu, Michael Zeng, and Lijuan Wang. Mm-react: Prompting chatgpt for multimodal reasoning and action. *arXiv preprint arXiv:2303.11381*, 2023b.
- Shunyu Yao, Jeffrey Zhao, Dian Yu, Nan Du, Izhak Shafran, Karthik Narasimhan, and Yuan Cao. React: Synergizing reasoning and acting in language models. In *International Conference on Learning Representations*, 2023.
- Yiyang Yao, Peng Liu, Tiancheng Zhao, Qianqian Zhang, Jiajia Liao, Chunxin Fang, Kyusong Lee, and Qing Wang. How to evaluate the generalization of detection? a benchmark for comprehensive open-vocabulary detection. In *AAAI Conference on Artificial Intelligence*, 2024.
- Qinghao Ye, Haiyang Xu, Guohai Xu, Jiabo Ye, Ming Yan, Yiyang Zhou, Junyang Wang, Anwen Hu, Pengcheng Shi, Yaya Shi, Chenliang Li, Yuanhong Xu, Hehong Chen, Junfeng Tian, Qi Qian, Ji Zhang, Fei Huang, and Jingren Zhou. mplug-owl: Modularization empowers large language models with multimodality. *arXiv preprint arXiv:2304.14178*, 2023.
- Yohei Nakajima. BabyAGI, 2023. URL <https://github.com/yoheinakajima/babyagi>.
- Haoxuan You, Haotian Zhang, Zhe Gan, Xianzhi Du, Bowen Zhang, Zirui Wang, Liangliang Cao, Shih-Fu Chang, and Yinfei Yang. Ferret: Refer and ground anything anywhere at any granularity. In *International Conference on Learning Representations*, 2024.
- Licheng Yu, Patrick Poirson, Shan Yang, Alexander C Berg, and Tamara L Berg. Modeling context in referring expressions. In *European Conference on Computer Vision*, 2016.
- Zishun Yu, Yunzhe Tao, Liyu Chen, Tao Sun, and Hongxia Yang. \mathcal{B} -coder: Value-based deep reinforcement learning for program synthesis. In *International Conference on Learning Representations*, 2024.
- Yuqian Yuan, Wentong Li, Jian Liu, Dongqi Tang, Xinjie Luo, Chi Qin, Lei Zhang, and Jianke Zhu. Osprey: Pixel understanding with visual instruction tuning. In *IEEE/CVF Conference on Computer Vision and Pattern Recognition*, 2024.
- Aohan Zeng, Xiao Liu, Zhengxiao Du, Zihan Wang, Hanyu Lai, Ming Ding, Zhuoyi Yang, Yifan Xu, Wendi Zheng, Xiao Xia, Weng Lam Tam, Zixuan Ma, Yufei Xue, Jidong Zhai, Wenguang Chen, Zhiyuan Liu, Peng Zhang, Yuxiao Dong, and Jie Tang. GLM-130b: An open bilingual pre-trained model. In *International Conference on Learning Representations*, 2023.
- Xiaohua Zhai, Basil Mustafa, Alexander Kolesnikov, and Lucas Beyer. Sigmoid loss for language image pre-training. In *IEEE/CVF International Conference on Computer Vision*, 2023.

- Hao Zhang, Feng Li, Shilong Liu, Lei Zhang, Hang Su, Jun Zhu, Lionel M. Ni, and Heung-Yeung Shum. Dino: Detr with improved denoising anchor boxes for end-to-end object detection. In *International Conference on Learning Representations*, 2023a.
- Haotian Zhang, Pengchuan Zhang, Xiaowei Hu, Yen-Chun Chen, Liunian Harold Li, Xiyang Dai, Lijuan Wang, Lu Yuan, Jenq-Neng Hwang, and Jianfeng Gao. Glipv2: unifying localization and vl understanding. In *Advances in Neural Information Processing Systems*, 2022.
- Pan Zhang, Xiaoyi Dong, Bin Wang, Yuhang Cao, Chao Xu, Linke Ouyang, Zhiyuan Zhao, Haodong Duan, Songyang Zhang, Shuangrui Ding, Wenwei Zhang, Hang Yan, Xinyue Zhang, Wei Li, Jingwen Li, Kai Chen, Conghui He, Xingcheng Zhang, Yu Qiao, Dahua Lin, and Jiaqi Wang. Internlm-xcomposer: A vision-language large model for advanced text-image comprehension and composition. *arXiv preprint arXiv:2309.15112*, 2023b.
- Tao Zhang, Xiangtai Li, Hao Fei, Haobo Yuan, Shengqiong Wu, Shunping Ji, Change Loy Chen, and Shuicheng Yan. Omg-llava: Bridging image-level, object-level, pixel-level reasoning and understanding. In *Advances in Neural Information Processing Systems*, 2024.
- Xiangyu Zhao, Yicheng Chen, Shilin Xu, Xiangtai Li, Xinjiang Wang, Yining Li, and Haian Huang. An open and comprehensive pipeline for unified object grounding and detection. *arXiv preprint arXiv:2401.02361*, 2024.
- Lianmin Zheng, Wei-Lin Chiang, Ying Sheng, Siyuan Zhuang, Zhanghao Wu, Yonghao Zhuang, Zi Lin, Zhuohan Li, Dacheng Li, Eric Xing, et al. Judging llm-as-a-judge with mt-bench and chatbot arena. In *Advances in Neural Information Processing Systems*, 2023.

APPENDIX OVERVIEW

We provide an overview to present a clear understanding of this section.

- In Sec. **A**, we provide an overview pipeline of the language data generation.
- In Sec. **B**, we show more examples of raw expressions corrected by our Real-LOD.
- In Sec. **C**, we present visual comparisons of existing LOD methods under various queries.
- In Sec. **D**, we illustrate several examples of how Real-LOD refines raw expressions.
- In Sec. **E**, we provide more evaluation results on the LOD benchmark.
- In Sec. **F**, we present a pseudo-code of proposed Real-LOD workflow.
- In Sec. **G**, we show prompts for LLM and VLM to execute different tasks.
- In Sec. **H**, we outline the specifics of the training, evaluation, datasets, and model structure.
- In Sec. **I**, we discuss the broader impact and limitations of our paper.
- In Sec. **J**, we provide more analytical experiment for Real-LOD.

A EXPRESSION GENERATION PIPELINE

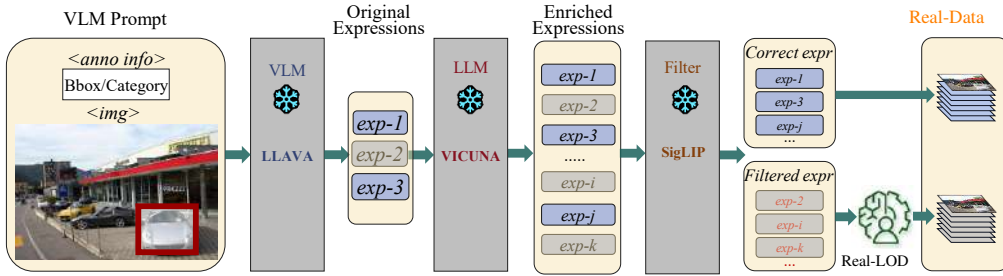


Figure 9: An overview of our language generation pipeline for **Real-Data**. In this pipeline, we first use VLM (LLaVA) to generate descriptions. For each object, we randomly select two prepared prompts presented in Tab. 8 with an image and corresponding category for LLaVA to generate expressions. Second, LLM (Vicuna) is introduced to generate synonyms to expand the number of expressions using the prompt in Tab. 8. We repeat the process two times for each expression. Then, we use the language-image match model (SigLIP) to filter expression-image pairs with low scores. Finally, we maintain correct data pairs and refine filtered expressions via our Real-LOD to build the final dataset **Real-Data**.

B RE-ALIGNMENT EXAMPLES OF REAL-LOD

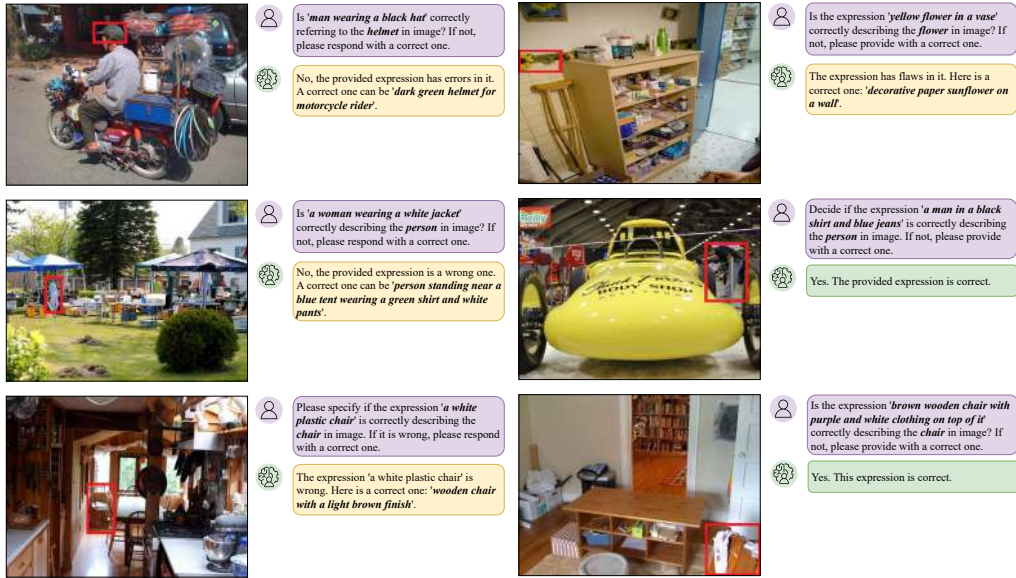


Figure 10: We show examples of the re-alignment by Real-LOD. Real-LOD can correct wrong expressions and remain correct ones.

C VISUAL COMPARISON RESULTS OF LOD MODELS

Query : “This item is used to keep warm in colder weather.”



Query : “Woman in wedding dress next to a man in suit.”



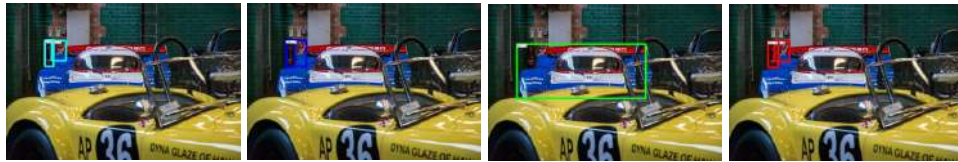
Query : “Pillow placed at the head of the bed.”



Query : “These two people each have a pink surfboard.”



Query : “The fire extinguisher on the left.”



Query : “Cows that are laid down.”



(a) GLIP-L

(b) APE-B

(c) mm-GDINO

(d) **Real-Model**

Figure 11: Visual comparison with existing language and vision detectors. The backbone of GLIP and APE-B is ViT-L, and the backbone of mm-GDINO is Swin-B. We use 0.3 as the score threshold for the fair comparison. For convenience, we use bboxes with different colors to distinguish each model. The color we used for **Real-Model** is red.

D EXAMPLES OF RE-ALIGNMENT BY REAL-LOD

In Fig. 12- 17, we show several examples of how Real-LOD works.



Figure 12: An example of how Real-LOD handles correct expressions.

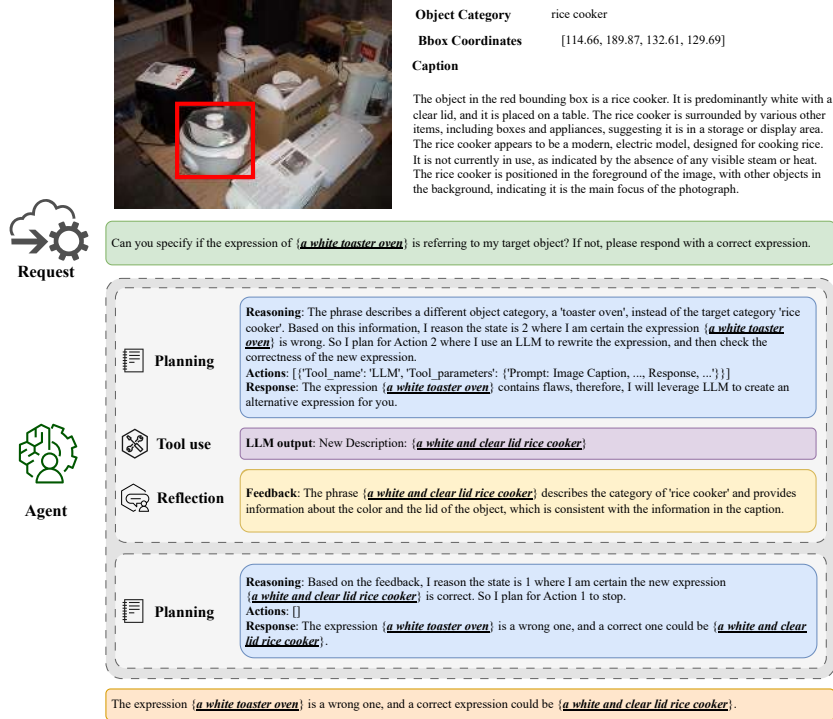


Figure 13: An example of how Real-LOD corrects a wrong expression. It consists 'Rewrite' action.

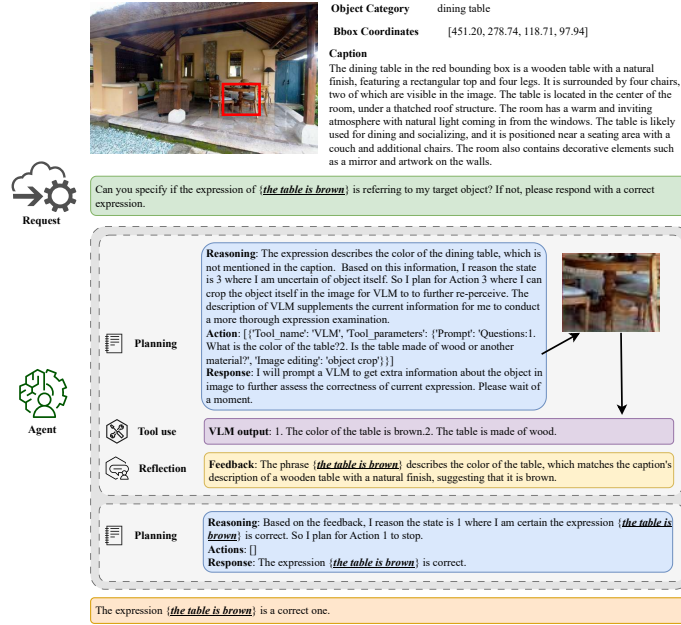


Figure 14: An example of how Real-LOD handles an uncertain expression. It consists 'VLM with object crop' action.

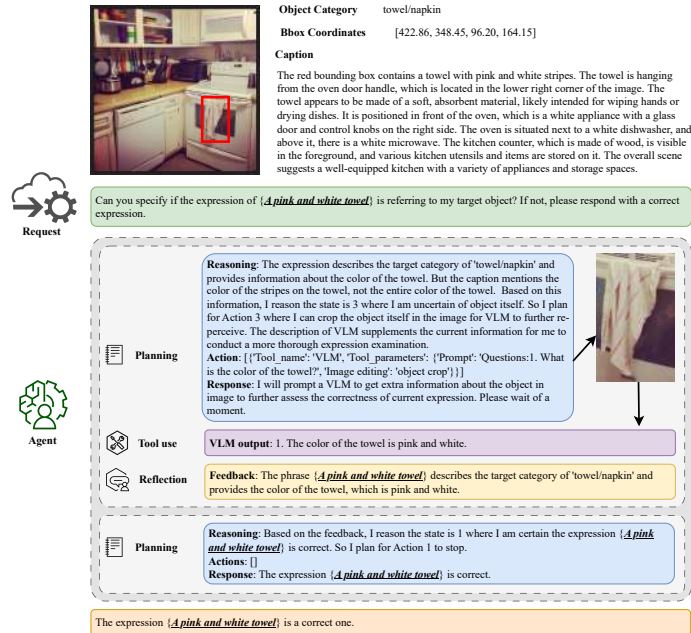


Figure 15: An example of how Real-LOD handles an uncertain expression. It consists 'VLM with object crop' action.

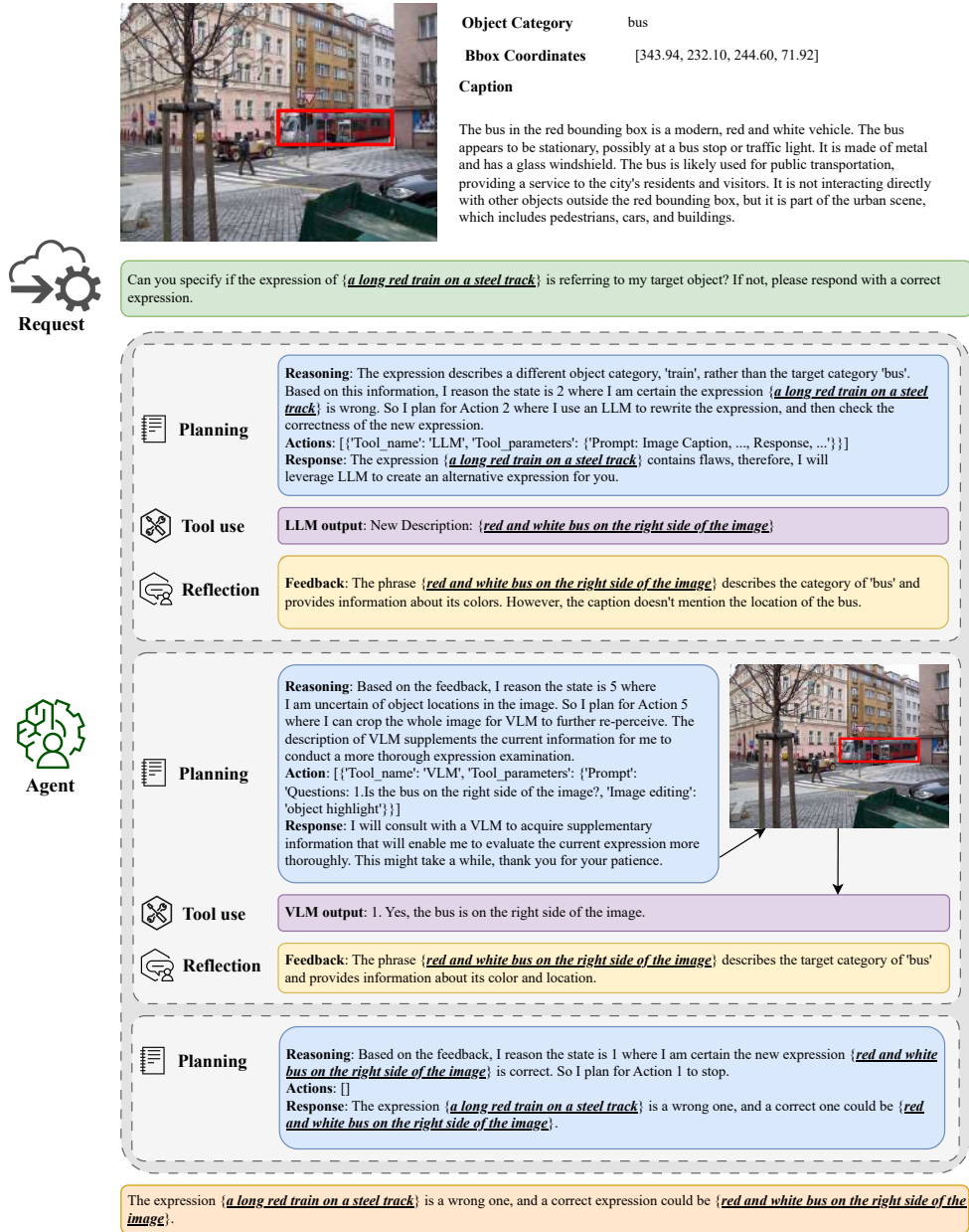


Figure 16: An example of how Real-LOD refines a raw expression. This workflow consists two actions ('Rewrite' and 'VLM with object highlight')

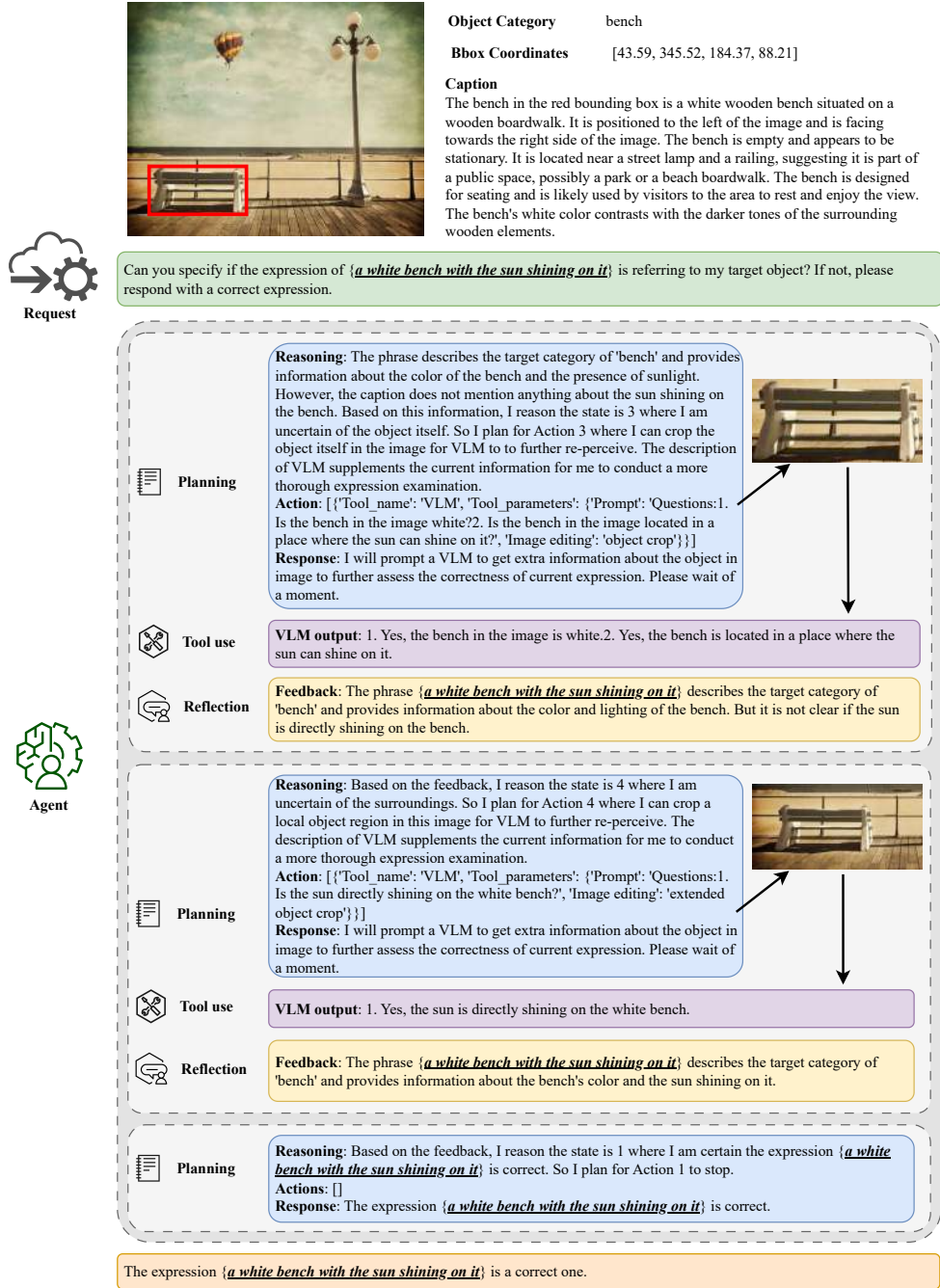


Figure 17: An example of how Real-LOD handles an uncertain expression. It consists ‘VLM with object crop’ and ‘VLM with extended object crop’ actions.

E ADDITIONAL EVALUATION RESULTS

E.1 APPLICATION TO OTHER LOD MODELS

In this subsection, we conduct experiments to demonstrate the generalization ability of our method. We apply our **Real-Data** to UNINEXT (Yan et al., 2023) and a tiny version of mm-GDINO (Zhao et al., 2024). We report the results of OmniLabel and DOD benchmarks in Tab. 5 and Tab. 5, respectively. For UNINEXT, the AP-des of OmniLabel and of DOD are significantly increased to 23.4% and 24.2% without adjusting any training parameters. Notably, we only train UNINEXT for five epochs based on a relatively small backbone (*i.e.*, ResNet-50). For mm-GDINO with a Swin-T backbone, the AP-des of OmniLabel and of DOD are significantly improved to 29.9% and 30.8%. The results demonstrate the holistic nature of our method.

Table 5: Application to other LOD models on OmniLabel benchmark.

Test subset	LOD method	BackBone	Real-Data	AP-des	AP-des-pos	AP-des-S	AP-des-M	AP-des-L
COCO	MM-GDINO (Zhao et al., 2024)	Swin-T		10.1	31.2	19.7	9.4	10.4
			✓	20.5	51.9	30.9	19.6	21.1
	UNINEXT (Yan et al., 2023)	ResNet-50		3.6	10.3	8.9	3.8	2.0
			✓	14.6	41.4	24.8	13.6	14.8
O365	MM-GDINO (Zhao et al., 2024)	Swin-T		16.1	24.7	32.7	12.7	7.9
			✓	29.6	44.4	49.0	26.2	19.6
	UNINEXT (Yan et al., 2023)	ResNet-50		7.6	13.9	10.8	8.1	4.6
			✓	24.3	38.2	37.7	21.3	17.3
OI	MM-GDINO (Zhao et al., 2024)	Swin-T		20.6	30.4	37.2	18.1	12.9
			✓	33.7	45.1	48.5	30.8	25.1
	UNINEXT (Yan et al., 2023)	ResNet-50		5.1	7.1	9.2	4.9	3.2
			✓	25.3	36.3	36.9	22.8	19.1
ALL	MM-GDINO (Zhao et al., 2024)	Swin-T		17.0	26.7	33.3	13.9	9.3
			✓	29.9	44.3	47.5	26.9	20.7
	UNINEXT (Yan et al., 2023)	ResNet-50		6.0	10.4	9.6	5.8	3.5
			✓	23.4	37.3	36.3	20.7	17.3

Table 6: Application to other LOD models on DOD benchmark.

LOD method	BackBone	Real-Data	Full	Presence	Absence
MM-GDINO (Zhao et al., 2024)	Swin-T		23.0	21.9	26.0
		✓	30.8	30.3	32.7
UNINEXT (Yan et al., 2023)	ResNet-50		10.7	10.6	10.9
		✓	24.2	23.2	26.9

E.2 COMPARISONS WITH STATE-OF-THE-ART LOD MODELS ON OVDEVAL BENCHMARK

In this subsection, we show evaluation results in OVDEval benchmark (Yao et al., 2024). The benchmark contains 15.1k images with 28.1k bbxs and 10.1k language expressions. The dataset is divided into several sub-dataset according to aspects such as ‘color’ and ‘relationship’. We select a language-based sub-dataset to compare our **Real-Model** model with other detectors. Tab. 7 shows the results. The OmDet method performs best in the ‘Relationship’ sub-dataset. The reason is that the testing data is collected from HOI (Chen et al., 2023b) dataset, which is used to train the OmDet model. Our **Real-Model** outperforms existing LOD models on average in this benchmark.

Table 7: State-of-the-art comparison on OVDEval benchmark. We report evaluation results AP (%) of each sub-dataset. ‘Source’ refers to the source of training images. ‘#Img’ refers to the number of images.

LOD method	Backbone	Source	#Img	color	material	Position	Relationship	Negation	Avg
GLIP (Li et al., 2022)	Swin-L	O365, OI, RefC/g+/, etc	17.5M	6.7	15.8	48.1	33.2	51.8	31.1
OmDet (Yao et al., 2024)	ConvNext-B	O365, GoldG, HOI-A, etc	1.1M	24.5	22.5	47.7	51.8	55.8	40.4
FIBER (Dou et al., 2022)	Swin-B	COCO, CC3M, SBU, etc	4M	9.4	17.7	48.1	33.2	58.1	33.3
Real-Model	Swin-B	Real-Data	0.18M	25.7	22.5	59.3	41.9	68.4	43.6

F ALGORITHM OF AGENTIC WORKFLOW

Algorithm 1 Pseudo code of Real-LOD. We show detailed code of our workflow in flexibly leveraging tools to re-align raw expressions to given objects.

Input: image I , object locations O , caption C , raw expression E_r
Output: re-aligned expression E_R

```

1: agent  $\leftarrow$  Real-LOD(init assistant, init vlm_tool, init llm_tool) //Agent initialization
2: info_pool  $\leftarrow$  {"image":  $I$ , ..., "expressions": [ $E_r$ ]} //Initialized as input
3: iteration  $\leftarrow$  0
4: stop  $\leftarrow$  False
5: solved  $\leftarrow$  False
6: while not stop do
7:   //Stage 1. planning based on current info_pool
8:   reasoning, actions, values  $\leftarrow$  agent.assistant
9:   //Stage 2. tool use and update info_pool
10:  if (actions is not empty) and (iteration < max_iter) then
11:    for action in actions do
12:      tool_name, tool_params  $\leftarrow$  action
13:      case tool_name is "VLM", update info_pool with agent.vlm_tool(tool_params)
14:      case tool_name is "LLM", update info_pool with agent.llm_tool(tool_params)
15:    end for
16:    //Stage 3. reflection on tool outputs
17:    update feedback with agent.llm_tool
18:    iteration  $\leftarrow$  iteration + 1
19:  else if actions is empty then
20:    solved  $\leftarrow$  True // reach a correct expression
21:  end if
22:  stop  $\leftarrow$  solved or (iteration == max_iter)
23: end while
24:  $E_R \leftarrow$  info_pool["expressions"][-1]
25: return  $E_R$ 

```

G PROMPTS FOR LLM AND VLM

G.1 PROMPTS FOR RAW EXPRESSION GENERATION

Prompts for VLM to generate raw expression

1. For the given image <image>, please provide a unique description for the <object> in the area <boxes>.
2. What is the content depicted of the <object> located in the area <boxes> of the image <image>?
3. Please describe the <object> in the area <boxes> of this image <image>.
4. I would like to know the description of the <object> in the area <boxes> of the picture <image>.
5. Kindly describe the <object> in the area <boxes> of the picture <image>.
6. Give me detailed descriptions of the <object> in area <boxes> of this image <image>, including its' color, material, attribute, etc.
7. What's the difference between <object> in area <boxes> and other <object> in this image <image>?

Prompt for LLM to diversify raw expression

I want you to act as a synonymous expression provider. I will give you a text of phrase or short sentence, which is an expression that describes a main object while mentioning some other objects. And you will reply to me with a new expression that have the same semantic meaning and describe the same main object as the provided expression. The new expressions should also be phrases or short sentences no longer than 25 words. Do not write explanations on replies. Do not repeat.

Table 8: Prompts for raw expression generation.

G.2 PROMPTS FOR REWRITE TASK

Task Description

You are an excellent text analyst and generator. I want a short text description that correctly describing my chosen object in an image. Now I already have one description but there might be mistakes in it and I want you to help with this. I will provide you with the following as background knowledge:

1. Image Caption: a caption describing the content in an image.
2. Chosen Object: one or more objects chosen in this image to describe and their corresponding coordinates. The top-left corner of the image has coordinates [0, 0] and the bottom-right corner has coordinates [1, 1]. Each object is represented as {'id': unique object identification, 'category name': object category, 'box':[top-left x, top-left y, box width, box height]}.
3. Other Object: other objects in image and their corresponding coordinates, which are provided to you in the same format as the 'Chosen Object'.
4. Object Description: a short text for you to analyse (this description could be correct, partially correct or wrong).

As an assistant, analyse the 'Object Description' and generate a 'New Description' based on it, which correctly describes the chosen object:

1. your new description should be centered on the chosen object, and describes the correct object category
2. your new description should be consistent with information provided by the given caption and with general knowledge
3. your new description should be a short phrase and has reasonable meaning

One In-context Example

Prompt: Image Caption: The image showcases a clean and well-organized kitchen with wooden floors and wooden cabinets. The kitchen features a white refrigerator, a sink with a window above it, and a stove with an oven below it. Additionally, there is a dishwasher and a washing machine in the kitchen. The appliances are neatly arranged, and the overall appearance of the kitchen is tidy and inviting.

Chosen Object: [{'id':0, 'category name':'Home appliance', 'box':[0.68, 0.52, 0.15, 0.05]}, {'id':1, 'category name':'Home appliance', 'box':[0.0, 0.26, 0.24, 0.74]}, {'id':2, 'category name':'Home appliance', 'box':[0.53, 0.56, 0.14, 0.28]}, {'id':3, 'category name':'Home appliance', 'box':[0.68, 0.22, 0.15, 0.06]}, {'id':4, 'category name':'Home appliance', 'box':[0.67, 0.57, 0.16, 0.21]}]

Other Object: []

Object Description: 'appliance for cleaning dishes with water and detergent'

Response: Reasoning: The description is centered on home appliance, but it only refers to the washing machine in the kitchen, which is only one of the chosen objects. The object category is 'home appliance', which also include the refrigerator, the sink and the stove mentioned in the given caption. So the description does not match all the objects belongs to 'home appliance' in the image. I can rewrite this description into a more specific one.

New Description: 'home appliances of refrigerator, sink, stove, dishwasher and washing machine'

Python code together with above text prompts are directly sent to LLM-for-Rewriting

```
messages = [{"role": system, "content": task_description}]
for example in in_context_examples:
    messages.append({"role": user, "content": example["prompt"]})
    messages.append({"role": assistant, "content": example["response"]})

content=f"Image caption: " + caption + "\n"
content+=f"Chosen Object: " + chosen_object + "\n"
content+=f"Other Object: " + other_object + "\n"
content+=f"Object Description: " + object_description + "\n"
messages.append({"role": user, "content": content})
```

Table 9: Task description and an in-context example for LLM-for-Rewriting tool. There are five in-context examples used in the text prompt, we show one example of them here for simplicity.

G.3 PROMPTS FOR REFLECTION

Task Description

You are an excellent text analyst. I want to get correct descriptions of a target object in an image. Now I already have a phrase describing this target object, but the texts might contain mistakes and I want you to help with this.

I will provide you with this phrase to be checked, along with a ‘Object Category’ and a ‘Caption’ as reference information:

1. Object Category: the exact category name of my target object.
 2. Caption: a long text describing content in the image, information provided in this caption is correct. Note that some details in the image might be missing in this caption.
- Given the reference information, your task is to verify if the phrase correctly describes my target object.

Process Instruction

1. Correct phrase: If the phrase describes the target category and provides similar information that can be found in the caption, this phrase is correct.
2. Uncertain phrase: If the phrase describes the target category but provides information that is missing in the caption, this phrase is uncertain. Please tell me what information in this phrase is not mentioned in the given caption. Extra information could be object color, object material, object location in the image, object action, object relation with other objects in image, etc.
3. Wrong phrase: If the phrase describes a different object category, or the phrase provides information that have conflicts with the caption, this phrase is wrong.

One In-context Example

Prompt: Object Category: Laptop

Caption: In the image, there are two women sitting at a table, both focused on their laptops. One of the women is holding up her middle finger, possibly as a gesture of defiance or humor. On the table, there is a bottle, a cup, and a laptop being used by one of the women. The woman with the laptop is wearing a scarf, and the other woman is positioned on the other side of the table. Drink: A clear plastic bottle of water is on the table. It is placed in front of the woman with the laptop. Laptop: The laptop is a black and silver Dell computer. The woman is using it while sitting at the table. Table: The table is a dining table where the woman is sitting with her laptop and a bottle of water. Bottle: The bottle is a clear plastic bottle of water. It is placed on the table in front of the woman with the laptop. Phrase: ‘black and silver Dell computer’

Response: Feedback: The phrase describes a computer and provides its color and brand. ‘Computer’ is similar with ‘Laptop’ and the caption claims the laptop in the image to be a black and silver Dell computer, this phrase is correctly describing the target object.

Python code together with above text prompts are directly sent to LLM-Reflector

```
messages = [{"role": system, "content": task_description}]
for example in in_context_examples:
    messages.append({"role": user, "content": example["prompt"]})
    messages.append({"role": assistant, "content": example["response"]})

content=f"Object Category: " + category + "\n"
content+=f"Caption: " + caption + "\n"
content+=f"Phrase: " + phrase + "\n"
messages.append({"role": user, "content": content})
```

Table 10: Task description and an in-context example for agent reflection. There are five in-context examples used in the text prompt, we show one example of them here for simplicity.

G.4 PROMPTS FOR RESPONSE GENERATION OF FINE-TUNING DATA

1. Generate question for uncertain state

Task Description

You are an excellent text analyst.

I have a phrase that describes an object in an image. I have already analyzed this phrase based on a caption. And I have reached the conclusion that this phrase is uncertain. I want you to help me generate questions asking about the missing information in the caption.

I will provide you with my statement of the reason why the phrase is uncertain. As an assistant, please analyse my statement and respond with your generated questions. Ask about the object in image only, do not involve the caption in your questions. Ask as few questions as possible.

One In-context Example

Prompt: Phrase: "a book with the word 'Fix' on it"

Reasoning: The phrase "a book with the word 'Fix' on it" describes the target category of 'book' and provides extra information that the word "Fix" is on the book. However, the caption does not mention any specific word on the book, so extra information is needed to determine if the phrase is correct.

Conclusion: The phrase is uncertain. The caption does not mention any specific word on the book, so it is unclear if the phrase is correct or not.

Response: Questions: 1. Is there any specific word on the book? If so, what is the word on the book?

2. Generate target object for action during uncertain state

Task Description

You are an excellent text analyst. I have a phrase that describes an object in an image. I have already analyzed this phrase based on a caption. And I have reached the conclusion that this phrase is uncertain. First, I want you to help me generate questions asking about the missing information in the caption. I will provide you with my statement of the reason why the phrase is uncertain. As an assistant, please analyze my statement and respond with your generated questions. Ask about the object in image only, do not involve the caption in your questions. Ask as few questions as possible.

Secondly, based on the questions you have generated, I want you to give me a target area where the miss information may most likely be found. Choose one receptive field from the following 3 options: 1) the object itself, 2) the object and the surrounding areas, 3) the whole image. Here are some hints for you. If the missing information is about some attribute of the object, such as colors, materials, the target area is likely the object itself 1). If the missing information is something interacting with the object, the target area is likely the object and the surrounding area 2). If the missing information is about another object, the target area is likely the whole image 3). Give me the number of the choice and only choose one target area per task.

One In-context Example

Prompt: Phrase: 'bread loaf on a tan bowl'

Reasoning: The phrase describes a large tan colored bowl with a bread loaf sitting in it. However, the caption does not mention the color or the presence of food in the bowl. The size of the bowl is also not mentioned.

Conclusion: The phrase is uncertain. The color of the bowl, the presence of food and the size of the bowl are not mentioned in the caption.

Questions: 1. What is the color of the bowl? 2. Is there any food in the bowl? If so, what type of food is in the bowl? 3. What is the size of the bowl? Is it small or large?

Response: Target area: 1) the object itself.

Table 11: Task description and an in-context example for response generation of fine-tuning data. There are five in-context examples used in each text prompt, we show one example of them here for simplicity. We omit the Python code together with text prompts, which is similar to Tab. 10 and Tab. 12.

G.5 VISUAL AND LANGUAGE PROMPTS FOR VLM

Language prompt

Here are some prior knowledge about this image. The object in image is a *{object category}*. There is a possible description of this image, it may not be precise enough: *{current expression}*. Answer the following questions. *{Questions generated by Real-LOD}*.

Visual prompt

Visual prompts of three actions for VLM:



Table 12: Visual and textual prompts for VLM tools. We show examples of the three image editing for VLM. Visual and language prompts are generated case by case via our Real-LOD.

H TECHNICAL DETAILS

H.1 LICENSES OF DATASETS, CODES AND MODELS

In Tab. 13, we present the Licenses and URL of datasets, codes and models used in our paper.

Table 13: The License and URL of datasets, codes and models utilized in this paper.

Assert	Type	License
O365 (Shao et al., 2019)	Dataset	Creative Commons Attribution 4.0 License.
OpenImage (Kuznetsova et al., 2020)	Dataset	-
LVIS (Gupta et al., 2019)	Dataset	Creative Commons Attribution 4.0 License.
Omnilabel (Schulter et al., 2023)	Dataset	MIT License.
DOD (Xie et al., 2023)	Dataset	Creative Commons Attribution 4.0 License.
OVD Eval (Yao et al., 2024)	Dataset	Apache-2.0 license.
Refcoco/g+ (Mao et al., 2016)	Dataset	Apache-2.0 license.
MMDetection (Chen et al., 2019)	Code	Apache-2.0 license.
ChatGLM (Zeng et al., 2023)	Code	Apache-2.0 license.
LLaVA (Liu et al., 2023a)	Model	Apache-2.0 license.
Vicuna (Zheng et al., 2023)	Model	Llama 2 Community License Agreement.

H.2 TRAINING DETAILS OF REAL-MODEL

The implementation of **Real-Model** is based on the MMDetection (Chen et al., 2019) framework and PyTorch (Paszke et al., 2019). The input size of all the experiments is 1333×800 , and the batch size is 4 per GPU. In the ablation study, there is only a single machine with 8 NVIDIA V100 GPUs for training to guarantee impartiality. For the final result, we train on 16 NVIDIA V100 GPUs for better performance. During training, we employ the AdamW optimizer (Kingma & Ba, 2017) with a momentum of 0.9 and a weight decay of 0.05. The learning rate setting includes a 1000-iteration warm-up with a start factor of 0.1 and a multi-step schedule with an initial value of 4×10^{-6} for 10 epochs. To be specific, the weights used for model initialization are referenced from the office repository of mm-GDINO (Zhao et al., 2024). We elaborate on our computation cost in Tab. 14 and provide the distribution of iteration numbers in Fig. 18.

Table 14: Computation cost in each step.

Step	Avg num of calls	Time cost of each call
Planning	3.09	0.265s
LLM-tool	0.65	0.131s
VLM-tool	0.43	0.159s
Reflection	2.08	0.291s

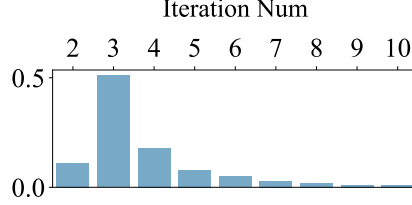


Figure 18: Distribution of iteration number.

H.3 EVALUATION DETAILS

In Tab. 15, we provide the detailed training data information of other LOD methods, which we compare within OmniLabel and DOD benchmark.

Table 15: A detailed list of training data information for other LOD methods.

LOD method	Backbone	Source	#Img
MDETR (Kamath et al., 2021)	ENB3	COCO, RefC/g/+, VG, GQA, Flickr30k	0.3M
GLIP (Li et al., 2022)	Swin-L	O365, COCO, OI, VG, ImageNet, GoldG, CC3M, CC12M, SBU	17.5M
FIBER (Dou et al., 2022)	Swin-B	COCO, CC3M, SBU, VG	4M
OWL-V2 (Minderer et al., 2023)	ViT-L	WebLI	10B
UniNext (Yan et al., 2023)	ViT-H	O365, RefC/g/+	0.7M
UniNext (Yan et al., 2023)	ResNet-50	O365, RefC/g/+	0.7M
GDINO (Liu et al., 2023c)	Swin-B	O365, OI, GoldG, CC4M, COCO, RefC/g/+	5.8M
OFA-DOD (Xie et al., 2023)	ResNet-101	CC12M, CC3M, SBU, COCO, VG, RefC/g/+	16M
APE-A (Shen et al., 2023b)	ViT-L	COCO, LVIS, O365, OI, VG	2.0M
APE-B (Shen et al., 2023b)	ViT-L	COCO, LVIS, O365, OI, VG, RefC/g/+	2.6M
mm-GDINO (Zhao et al., 2024)	Swin-T	O365, GoldG, GRIT, V3Det	2.8M
mm-GDINO (Zhao et al., 2024)	Swin-B	GoldG, O365, COCO, OI, RefC/g/+, V3Det, LVIS, GRIT	12M

H.4 MODEL DETAILS

In Fig. 19, we present more architectural details of the **Real-Model**, which is based on the mm-GDINO (Zhao et al., 2024). As shown in Fig. 19, the text encoder and image encoder first extract the text feature and image feature, respectively. The bidirectional feature enhancement module is then used to integrate the text and image features through cross-modality cross-attention. After integration, cross-modality queries are extracted from the image features with the language-guided query selection module and then subsequently input into the decoder with a further cross-modality fusion. The final output queries are then utilized for contractive loss and localization loss. More details can be found in (Yang et al., 2023b; Zhao et al., 2024).

I BROADER IMPACT AND LIMITATION

I.1 BROADER IMPACT

Agent and language-based object detection have shown significant applications in various real-world scenarios, particularly in intelligent robotics and autonomous driving. Our proposed method exhibits potential for these two research areas, offering valuable insights to the community. Our method focuses on correcting language expressions for the LOD dataset without a specific application goal. Hence, it does not directly involve societal issues.

I.2 LIMITATION

Real-LOD employs the visual-language model to perceive the content of a given target in various scenes, providing external information to help the linguistic descriptions correcting process for

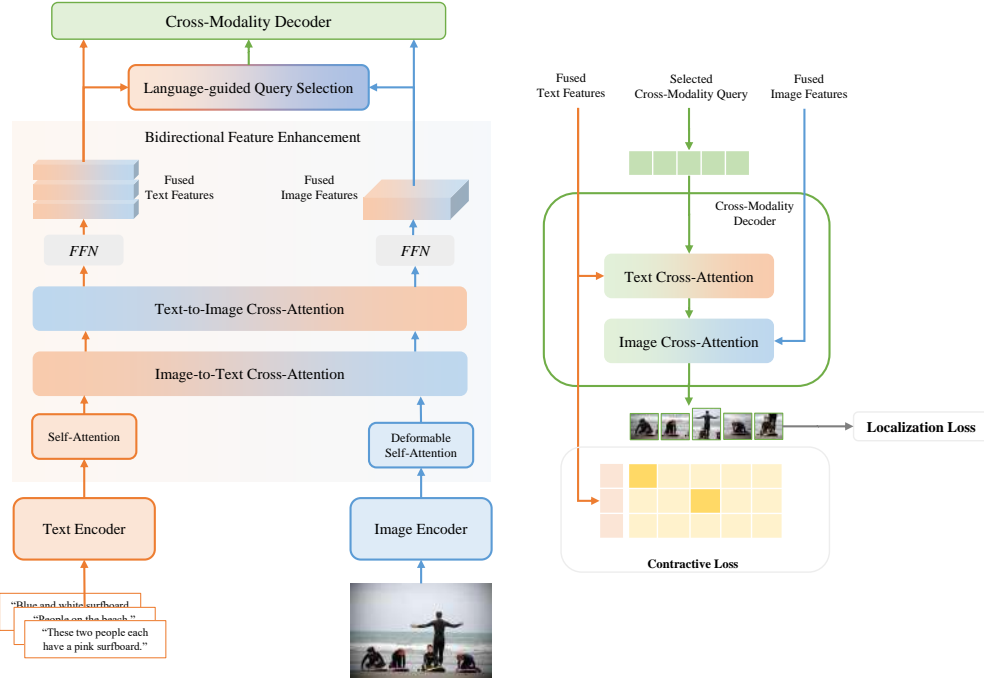


Figure 19: More architectural details of the **Real-Model**. The **Real-Model** is built upon the mm-GDINO (Zhao et al., 2024) and trained with **Real-Data** re-aligned with Real-LOD. The right part is the overall framework before the cross-modality decoder. The left part is the cross-modality decoder and loss calculation.

reducing the model hallucination. Although our method strongly stimulates the potential of VLMs by introducing agentic workflows and visual tools, there are still some unmanageable hard cases limited by the original performance of VLMs. As shown in Fig 20, there are two main kinds of data refinement error caused by the error perception of VLM:

1. Typical visual hard cases. As illustrated in Sec I.2 of the appendix, object-detection datasets include low-light or low-quality scenes and extremely small or difficult-to-recognize objects. It could be difficult for VLM to generate appropriate expressions for these targets.
2. Expression describes a foreground object instead of the target background object. VLM may ignore the target object in the background when an occlusion exists. In order to ensure high quality at the bbox level, the reflection module regards these expressions as wrong.

When conducting large-scale data refinement, we set the maximum iteration to 4. With several extra iterations, some failure cases are likely to be solved. Since we already have a large amount of high-quality data for downstream training with a task-solved rate of 75%, we choose not to increase this parameter for the sake of efficiency. This indicates the requirement of developing more powerful and robust VLMs to handle complicated situations more efficiently.

**Case 1. Small and blurry object****Object category:** desk**Latest expression:** person in red jacket holding white coffee cup**Case 2. Object in low-light area****Object category:** red cabbage**Latest expression:** purple sticker on banana**Case 3. Expression describes foreground object****Object category:** car**Latest expression:** white glass window on a building

Figure 20: Visualization of some failure cases.

J MORE ANALYTICAL EXPERIMENT

Table 16: Accuracy in choosing the corresponding state/action on the validation set of fine-tuning data (1k samples). The results demonstrate that our agent can accurately reason the state/action, especially for the "Wrong" and "Uncertain" states. In addition, the relatively lower accuracy of the "Correct" state indicates that our agent is strict with the quality of expression to prevent the hallucinations as much as possible.

State/Action	Accuracy
Correct/Stop	93.1%
Wrong/LLM	99.4%
Uncertain/Object Crop	99.6%
Uncertain/Extended Object Crop	95.8%
Uncertain/Highlight	90.0%

Table 17: More detailed ablation study of our agentic workflow. The details of the experimental setup can be found in Sec. 3.3. In the following table, the "w/o Planning" is the same as the random selection schema in Sec. 3.3. "w/o Cyclic Workflow" indicates the workflow with only one cycle. The results intuitively illustrate the importance of each component to our agentic workflow.

State/Action	Success Rate
Real-LOD	74.7%
w/o Planning	35.6%
w/o Action 2	18.0%
w/o Action 3	53.0%
w/o Action 4	51.8%
w/o Action 5	57.4%
w/o Cyclic Workflow	60.7%